AD-A128 412 MULTISENSOR APPROACHES FOR DETERMINING DEFLECTIONS OF THE VERTICAL(U) ANALYTIC SCIENCES CORP READING MA W G HELLER ET AL. JAN 83 TASC-TR-4051-2 ETL-0314 1/1

UNCLASSIFIED DAAK70-82-C-0011 F/G 8/5 NL

END
DATE FILMED
6-83
DTIC

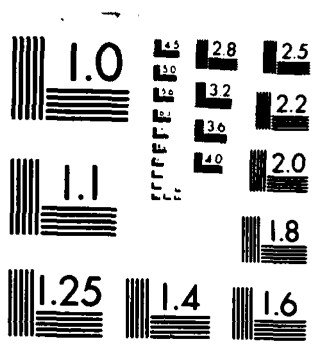

MICROCOPY RESOLUTION TEST CHART
NATIONAL BUREAU OF STANDARDS 1963-A

ETL-0314

AD-A128412

Multisensor approaches for determining deflections of the vertical

W. G. Heller

K.B. MacNichol

The Analytic Sciences Corporation
One Jacob Way
Reading, Massachusetts 01867

JANUARY 1983

Approved for Public Release. Distribution Unlimited.

Prepared For
U.S. ARMY CORPS OF ENGINEERS
ENGINEER TOPOGRAPHIC LABORATORIES
FORT BELVOIR, VIRGINIA 22060

E T L

ARMY ENGINEER TOPOGRAPHIC LABORATORIES
ETL

UNCLASSIFIED

SECURITY CLASSIFICATION OF THIS PAGE (When Data Entered)

REPORT DOCUMENTATION PAGE		READ INSTRUCTIONS BEFORE COMPLETING FORM
1. REPORT NUMBER ETL-0314	2. GOVT ACCESSION NO. AD-A128 412	3. RECIPIENT'S CATALOG NUMBER
4. TITLE (and Subtitle) Multisensor Approaches for Determining Deflections of the Vertical		5. TYPE OF REPORT & PERIOD COVERED Final Technical Report (1 Dec 1981 to 31 Dec 1982) 6. PERFORMING ORG. REPORT NUMBER TR-4051-2
7. AUTHOR(s) W.G. Heller K.B. MacNichol		8. CONTRACT OR GRANT NUMBER(s) DAAK70-82-C-0011
9. PERFORMING ORGANIZATION NAME AND ADDRESS The Analytic Sciences Corporation One Jacob Way Reading, Massachusetts 01867		10. PROGRAM ELEMENT, PROJECT, TASK AREA & WORK UNIT NUMBERS
11. CONTROLLING OFFICE NAME AND ADDRESS U.S. Army Engineer Topographic Laboratories Fort Belvoir, VA 22060		12. REPORT DATE January 1983 13. NUMBER OF PAGES
14. MONITORING AGENCY NAME & ADDRESS (if different from Controlling Office)		15. SECURITY CLASS. (of this report) UNCLASSIFIED 15a. DECLASSIFICATION/DOWNGRADING SCHEDULE

16. DISTRIBUTION STATEMENT (of this Report)

Approved for public release; distribution unlimited

17. DISTRIBUTION STATEMENT (of the abstract entered in Block 20, if different from Report)

18. SUPPLEMENTARY NOTES

19. KEY WORDS (Continue on reverse side if necessary and identify by block number)

Deflection of the Vertical	Multisensor	Astrolabe
Astrogeodetic surveys	Astrogravimetric	Theodolite
Gravity anomalies	Gradiometer	
Gravimetric techniques	Inertial Survey	

20. ABSTRACT (Continue on reverse side if necessary and identify by block number)

This final report documents the second phase of a study of methods for determining deflections of the vertical. In this phase multisensor techniques involving astrogeodetic, gravimetric, inertial, and gradiometric methods have been examined. The combination approaches discussed herein are those found to offer most promise in terms of accuracy, logistical convenience, and/or cost. Specific techniques treated in detail

DD FORM 1 JAN 73 1473 EDITION OF 1 NOV 65 IS OBSOLETE

UNCLASSIFIED

SECURITY CLASSIFICATION OF THIS PAGE (When Data Entered)

20. Abstract (Continued)

are the astrogeodetic method approached from a minimum variance estimation context, alternative moving base measurement techniques using supplemental astrogeodetic data, and regional adjustment of multiple tracks of inertial survey system measurements. Cost and logistical considerations for key single and multisensor deflection determination alternatives are reviewed.

PREFACE

This document is the final technical report, prepared under contract DAAK70-82-C-0011 for the U.S. Army Engineer Topographic Laboratories, Fort Belvoir, VA. The contracting officer's technical representative is Mr. William A. Allen, ETL-TD-EA.

TABLE OF CONTENTS

TABLE OF CONTENTS (Continued)

LIST OF FIGURES

LIST OF TABLES

1. INTRODUCTION

1.1 BACKGROUND

The development of high precision self-contained inertial navigation systems over the past two decades has made possible rapid positioning and gravity surveys. Such survey tools are used in both airborne and land-based configurations. Gravity quantities can be estimated with moderate accuracy using appropriate models and modern data processing techniques in conjunction with the inertial survey data. Gravity gradiometers, operating independently, or with an inertial navigation system, promise greater estimation accuracy in comparison to that obtained by conventional inertial systems. Even more accurate, but slower and more difficult to use for wide area coverage, is the astrogeodetic methodology for determining deflections of the vertical.

Accurate point estimates can be obtained for the gravity anomaly using gravimeters. Because deflections can be computed from fields of anomaly data, gravity measurements are also an approach to determining deflections of the vertical.

Little attention, however, has been given to the accuracy potential derived from processing multisensor data from the varied sources described above. Also, the accuracy improvement obtained by optimally combining multitrack data from moving base inertial systems has yet to be fully explored. More investigative efforts must be directed towards post-survey optimal processing techniques to extract the maximum information from all measurements made in a survey area. These issues are addressed in this report.

1.2 PURPOSE AND SCOPE

An assessment of the accuracy potential using high precision inertial systems with or without gravity gradiometers to estimate gravity disturbance quantities was performed in Ref. 1. In Ref. 2, the use of astrogeodetic or gravimetric data, in a single sensor, multimeasurement context, to estimate deflections of the vertical, was considered. Documenting the second phase of that effort, this report explores the accuracy realizable by optimally processing astrogeodetic data alone or in combination with gravimetric data. In addition, the qu ity of deflection estimates which are achievable by combining lti-track data from inertial and gradiometric systems with ast - geodetic data, is analyzed. Tradeoffs between accuracy a - able and survey effort (e.g., number of measurements) are made. Decision making parameters are identified, with emphasis on accuracy, cost and development time. Summaries of these findings are presented in Tables 4-1 and 4-2. The quantities of interest are deflections of the vertical and rms deflection estimation errors.

Deflection of the vertical recovery accuracies are reported for two types of survey scenarios,

- Astrogravimetric Survey
- Astrogeodetic/Moving Base Inertial Systems Survey.

Astrogeodetic measurements combined with gravimetric measurements in a defined area make up the astrogravimetric survey. In the second survey type, multitrack data from an inertial system and astrogeodetic measurements are combined to provide improved deflection estimates between astro stations. Although the multitrack aspect of the inertial survey investigations was

beyond the original scope which TASC had intended to pursue in this study, it became evident that meaningful comparisons among survey alternatives required that inertial surveys be treated in the same context as those providing astrogeodetic and gravimetric data. This context involves a rigorous treatment of minimum variance processing techniques applied to data taken in two-dimensions.

Three types of moving base inertial systems are studied in this effort. They are: a conventional inertial system (the baseline of Ref. 1, representative of the Rapid Gravity Survey System [RGSS]), a star tracking inertial system (the Northrop NAS-26 astroinertial navigator), and a moving-base gravity gradiometer system. The use of the Ref. 1 baseline scenario, a helicopter traverse over a straight, 35 km track, is maintained in this portion of the study for those cases involving survey tracks. Thus comparisons with the previous single track results are most meaningful. Note that actual data is not processed or analyzed in this report. Only the estimation accuracy potential of the methods for the defined survey arrangements is determined.

1.3 OVERVIEW OF REPORT

This report is organized as follows: Chapter 2 discusses the deflection estimation accuracy associated with astrogravimetric surveys. Chapter 3 addresses the astrogeodetic/moving base survey configurations. Costs and logistical issues are considered in Chapter 4 which also extends to a summary of important single sensor technological alternatives, for determining deflections of the vertical. A summary is provided in Chapter 5.

2. ASTROGRAVIMETRIC SURVEYS

2.1 INTRODUCTION

In this chapter the residual error in the estimate of the deflection of the vertical at a point, given measurements of both the deflection and gravity anomaly in the vicinity of the point and an appropriate worldwide gravity data base, is determined. This is performed by simulating the errors in measuring the various astrogeodetic and gravimetric quantities. In the actual processing algorithm, the measurements, consisting of astrogeodetic and gravimetric data taken over a specified survey area, are optimally combined to yield the desired deflection estimates. Since anomaly and deflection are correlated to some degree over the survey area, the combination of both types of measurements results in final error residuals which are smaller than those derived from either measurement alone. The numerical results presented here quantify the degree of improvement obtained by mixing astrogeodetic and gravimetric measurements in an optimal scheme and define the survey effort required to achieve a specific accuracy goal. The sensitivity of the residual errors to such factors as survey area geometry and gravity field characteristics is determined and provides insight into the advantages of this survey strategy.

In the next section the simulation models used in the analysis are presented and described. These include the gravity field models and the sensor (measurement) error models. A description of the survey area geometry is given in Section 2.3 and the methodology employed in determining the error residuals is detailed in Section 2.4. Numerical results of this portion of the study are presented in Section 2.5.

2.2 SIMULATION MODELS

The mathematical models developed in this report are statistical descriptions of random processes. As such they are used to describe the ensemble or average behavior of the quantities modeled. Auto- and cross-correlation matrices used in the numerical formulation are computed from analytic expressions for the correlation functions. Frequency domain descriptions (power spectral densities) are also employed.

2.2.1 Gravity Disturbance Models

The third-order Markov* analytic gravity model described and used in Ref. 1 (see also Ref. 4) is retained for the Phase II studies to characterize the gravity disturbance field (raw field). However, for the astrogravimetric portion of the studies, the model parameters have been modified to account for distant zone data as described below.

It is assumed that appropriate data from the DMA gravity library data base is to be used for "distant zone" coverage when processing gravimetric surveys. This data is available as area means in one deg × one deg blocks all over the world, and at smaller intervals in some specific areas. In ocean areas, the DMAAC data base includes the satellite altimetery information provided by GEOS-3 and SEASAT-1. For the (present) purpose of performing a survey effort and estimation accuracy assessment, the statistics of the anomaly errors are modeled. These are based on tabulated uncertainty estimates which are maintained as part of the gravity data base. In Ref. 3, numerical models are developed to represent the power spectral density of the free-air anomaly uncertainty. Separate representa-

*The model is "Markov", i.e., single step predictive/recursive, for processes modeled along a single track.

tions are developed for (1) the entire data base, yielding a world-wide (WW) model, and (2) for data in and near the Continental U.S. (CONUS) only, a CONUS model.

The self-consistent,* third-order Markov formulation of the WW and CONUS models also provides some important computational advantages over the numerical models of Ref. 3, the major one being that the auto- and cross-correlation for deflections of the vertical and anomaly are analytically computed (as a function of geometry) from simple formulas tabulated in the cited references. For the astrogravimetric survey the acf (autocorrelation function) form of the model is applicable, as opposed to the state-space form needed for temporal models (e.g., inertial navigation system simulation).

The anomaly power spectral density (PSD) function for the third-order Markov model is given by

$$\Phi_{gg}(\omega) = \frac{15\pi\ \beta^3\ \sigma_g^2\ \omega^2}{(\beta^2 + \omega^2)^{7/2}} \qquad (2.2\text{-}1)$$

where,

ω ~ two-dimensional radial spatial frequency (rad/km)

β ~ corner frequency (inverse of characteristic distance)

σ_g ~ rms value of the gravity anomaly

The two-dimensional PSD given by Eq. 2.2-1 is needed since gravimetric uncertainty in the entire horizontal plane is to be determined. The "corner frequency", or its inverse, the characteristic distance, divides the gravity anomaly spectrum

*Self-consistency is discussed at length in Ref. 4.

into two regions. Most of the anomaly energy occurs at frequencies, $\omega<\beta$. Anomaly frequencies greater than β contain decreasing amounts of energy. Hence, a long characteristic distance (low corner frequency) implies a gravity disturbance field which varies slightly over short distances while a short characteristic distance (high corner frequency) implies a gravity field which changes rapidly over short distances. The former characteristics are more desirable from an estimation viewpoint, since, for a gravity disturbance field which varies only slightly over short distances, an estimate of a gravity quantity at a point, given nearby measurements, can be made with reasonable certainty. However, for a field which varies significantly over short distances, this uncertainty is larger, since less information can be obtained from the measurements.* The post-measurement estimation uncertainty approaches that of the reference field for very short anomaly characteristic distances.

The parameters of the third-order Markov model can be selected to represent either the worldwide or the CONUS gravity anomaly models of Ref. 3. These parameter values are listed in Table 2.2-1.

TABLE 2.2-1
GRAVITY DATA BASE UNCERTAINTY MODEL PARAMETERS

PARAMETER	VALUE	
	WW MODEL	CONUS MODEL
σ_g (mgal)	38	14
β^{-1} (km)	35	16

*An extreme version of this situation occurs in mountainous terrain. Even when dense gravity data is available, adequate treatment requires additional information in the form of topography models. Modern thinking in this regard is set forth in Ref. 7.

2.2.2 Sensor Error Models

The data processing technique, described in Section 2.3, requires statistical descriptions (covariance matrices) of the measurement errors to compute the estimates and their error statistics. Error models are defined for the astrogeodetic and gravimetric measurements which comprise the astrogravimetric survey. Simple models have been chosen, but the parameter values are representative of actual measurement processes (Ref. 2). These are theodolite measurements and gravimeter measurements reduced to the geoid.

A first-order Markov noise model is used to describe the astrogeodetic measurement errors. The autocorrelation function of this process is given by

$$\phi(x) = \sigma^2 e^{-x/d} \tag{2.2-2}$$

where σ^2 is the variance, x is the shift distance, and d is the correlation distance. This model accounts for spatial correlations between astro measurements at different sites.*

Gravity anomaly measurement errors are modeled using a white noise description. The appropriate random process is described by

$$\phi(x) = A\,\delta(x) \tag{2.2-3}$$

where A is the strength of the process, x is the shift distance, and δ is the Dirac impulse function.

*An example of one correlation mechanism is anomalous atmospheric refraction. Weather cells or local conditions can cause similar refraction-induced errors over areas of one km or more.

A summary of the instrument (measurement) error models is provided in Table 2.2-2. Values for the error model parameters used in the present study are also listed. The anomaly error includes the effects of reduction and downward continuation of gravimeter measurements to the geoid.

TABLE 2.2-2
SENSOR ERROR MODELS

SENSOR (MEASUREMENT)	MODEL	PARAMETER VALUES
Astrogeodetic Deflection of the Vertical	First-Order Markov	0.3 $\widehat{\sec}$ rms correlation distance = 1 km
Gravimeter (Anomaly)	Uncorrelated post-survey reduction errors	1 mgal

2.3 SURVEY GEOMETRY

The astrogravimetric survey geometry, shown in Fig. 2.3-1, is a square pattern of measurement points in the horizontal plane. It represents either a very local survey or a "cell" which can be repeated over a large area. Astrogeodetic measurements (North and East) are made at the corners of the cell and may or may not be made at the cell midpoint. Deflection of the vertical survey error is evaluated at the center of the cell. The simulation studies address an arbitrary number of gravity anomaly measurements distributed over the area of the cell; nine are illustrated in Fig. 2.3-1. The number of anomaly measurements (e.g., the densification of anomaly data) is varied in the analysis to observe the change in the midpoint deflection of the vertical residual error for a given astro-measurement spacing.

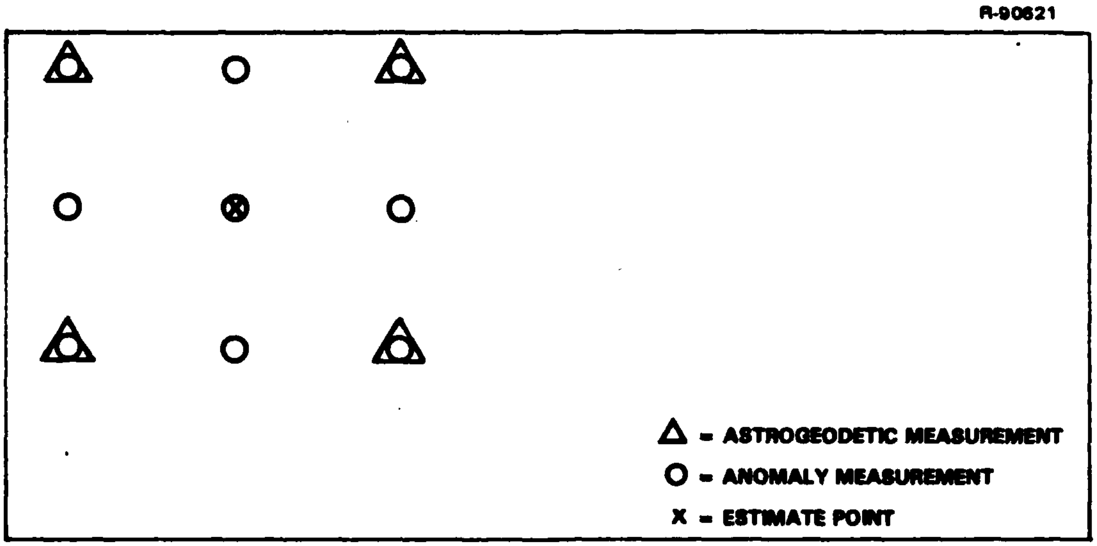

Figure 2.3-1 Typical Survey Geometry

2.4 ACCURACY EVALUATION METHODOLOGY

The analysis herein is based on the use of optimal (minimum variance) data processing techniques to estimate gravity quantities from zero mean field measurements. In this respect a vector quantity $\underline{x}$ is estimated from a vector of measurements $\underline{z}$ by

$$\hat{\underline{x}} = \phi_{xz} \phi_{zz}^{-1} \underline{z} \qquad (2.4\text{-}1)$$

where

ϕ_{xz} = cross-covariance between $\underline{x}$ and $\underline{z}$

ϕ_{zz} = covariance of $\underline{z}$

The covariance of the associated residual estimation errors is then computed from

$$\phi_{\tilde{x}\tilde{x}} = \phi_{xx} - \phi_{xz}\,\phi_{zz}^{-1}\phi_{zx} \qquad (2.4\text{-}2)$$

where ϕ_{xx} is the a priori covariance of $\underline{x}$.

If measurements ($\underline{z}$) of $\underline{x}$ are made, then

$$\phi_{zz} = \phi_{xx} + R_x \qquad \text{and } \phi_{xz} = \phi_{xx}$$

where R_x is the measurement error covariance matrix. This processing technique, also known as spatial collocation (see Ref. 5), forms the basis for the accuracy analysis performed here. Its main advantages are:

- Minimum variance estimates are determined
- No restrictions are placed on the spacing or locations of measurement or estimation points
- Systematically incorporates multisensor data
- Computationally efficient for a moderate number of measurements.

A more elaborate extension of this formulation involves computing the Fourier transforms of the quantities in Eq. 2.4-2 and performing the computations in the frequency domain. In this way the measurement covariance matrix to be inverted becomes diagonal, thereby streamlining the computations for large numbers of measurements. Such a method is described in Ref. 6. For the purposes of this study, however, spatial collocation is adequate.

The covariance matrices of Eq. 2.4-2 are analytically computed from the third-order Markov expressions tabulated in Ref. 4 for deflections of the vertical and gravity anomaly.

As previously discussed, the free parameters are chosen to fit the Markov model to the specified reference models of Ref. 2 (world-wide or CONUS). The survey geometry defines the vector distances between measurement and estimation points, and these distances are used to construct the covariance matrices. The measurement error covariance matrices are computed from the error models of Section 2.2.2.

Equation 2.4-2 may be solved once for all of the measurements, astrogeodetic and gravimetric, in a batch formulation. However, it is more informative to use the sequential collocation formulation of Ref. 5 to process the data in a sensor by sensor manner. In this way the accuracy effects of one measurement type, say, of anomaly, can be seen with respect to the impact of other measurement types (i.e., East and North deflections of the vertical). The sequential collocation formulas for three measurements are given in Appendix A.

2.5 NUMERICAL RESULTS

The accuracy evaluation methodology outlined in Section 2.4 is exercised here to quantify the performance potential of the application of the astrogravimetric method using minimum variance estimation. The simulation models of Section 2.2 are employed for a number of survey geometry variations and measurement schemes to determine the survey conditions required to achieve a specific accuracy goal. In this study, the survey cell midpoint serves as the accuracy evaluation point, and, for making comparisons and tradeoffs, a baseline accuracy goal of 0.2 $\widehat{sec}$ for the deflection estimate is established.

It is remarked in Section 2.2.1 that the estimation accuracy of a geopotential quantity, given nearby measurements, is particularly sensitive to the high frequency content of the

gravity disturbance field. This is shown in Fig. 2.5-1 where the deflection estimation uncertainty at the cell midpoint is plotted as a function of normalized characteristic distance. The normalization used is the characteristic distance of the worldwide gravity disturbance data base model. Note that, in Fig. 2.5-1, the world wide gravity disturbance characteristic distance, β_{ww}^{-1}, is taken from Table 2.2-1.

Increasing the model characteristic distance is mathematically equivalent to moving the measurements closer together. For example, if τ were decreased to 5 km, the appropriate abscissa in Fig. 2.5-1 would be 2. In the limit of zero spacing (or equivalently, infinite characteristic distance) the error quantity is a bias and the residual error of the estimate is simply the (uncorrelated) measurement error divided by the square root of the number of measurements. In the range of cases described by Fig. 2.5-1, the measurement error for each of the deflection measurements is 0.3 $\widehat{sec}$ and the astro-measurement error correlation distance is small compared to the measurement spacing (the astro-measurement errors are effectively uncorrelated with each other). Therefore all of the curves of Fig. 2.5-1 approach 0.15 $\widehat{sec}$ as the gravity model characteristic distance increases.

The number of anomaly measurements involved is also a simulation parameter. As indicated in Fig. 2.5-1, the number of anomaly measurements is important in reducing the deflection estimation uncertainty when the gravity disturbance field contains significant short wavelength energy. For gravity disturbance fields with modest short wavelength content, nearby anomaly measurements are of little benefit. A deflection estimate receives maximum information from an anomaly measurement when the two points are separated by about one characteristic distance. This aspect is typified by the small local minimum in the bottom curve of Fig. 2.5-1.

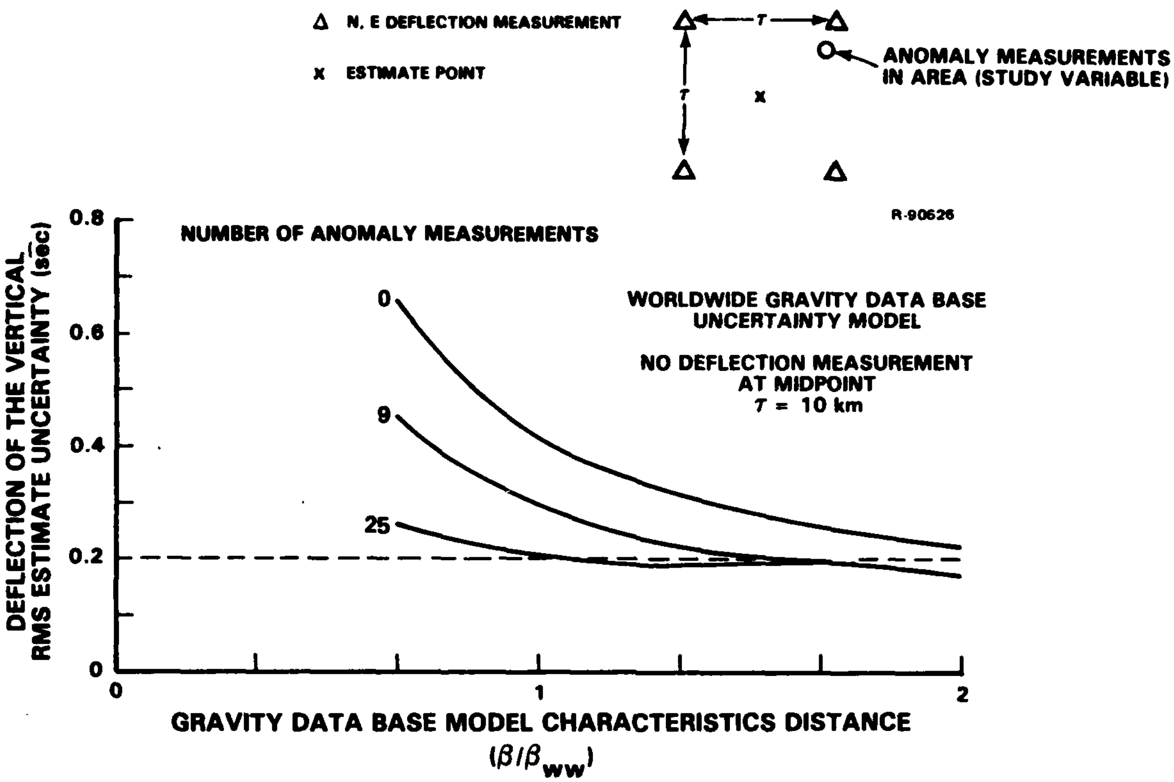

Figure 2.5-1 Sensitivity of Deflection of the Vertical Estimate Uncertainty to Gravity Disturbance Field Characteristic Distance

An important factor in determining astrogravimetric survey effort requirements involves the tradeoff between the deflection measurement spacing and gravimeter measurement densification within the survey area. The variations of the midpoint North deflection residual error (rms) with these factors are summarized in Fig. 2.5-2 using the worldwide gravity data base uncertainty model with no astrogeodetic measurements at the estimate point. It is clearly seen that a larger astro data spacing can be tolerated at the expense of increased densification of the gravimetric measurements. No anomaly data is required to achieve the estimation accuracy goal if the astro-measurement spacing is small. As the astro measurement

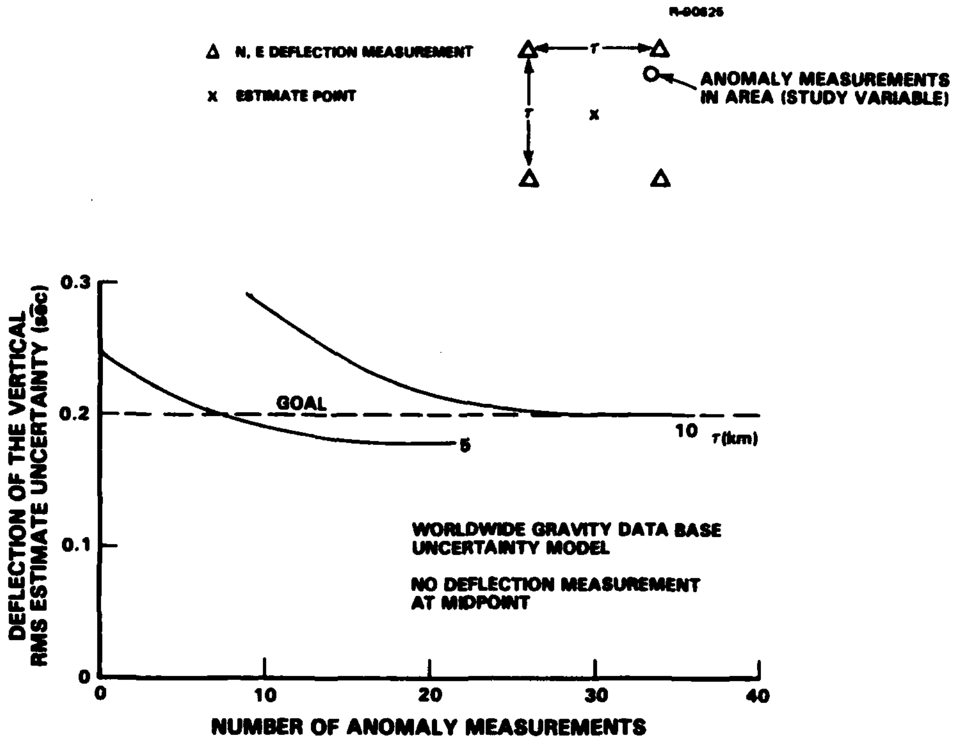

Figure 2.5-2 Alternative Astrogravimetric Measurement Strategies without Midpoint Deflection Measurement

separation distance increases, an increasing number of anomaly measurements are required to achieve the goal. If the astro-measurement spacing is large, then no reasonable number of anomaly measurements will result in the specified accuracy level. Fewer gravimetric measurements are required, or alternatively, larger astro-measurement spacings can be used if deflection measurements are made directly at the estimation point. This is shown in Fig. 2.5-3.

Similar graphs are presented in Figs. 2.5-4 and 2.5-5 for the CONUS gravity reference field. The results illustrated in Figs. 2.5-4 and 2.5-5 are indicative of typical astrogravimetric survey performance to be expected on the U.S. land mass.

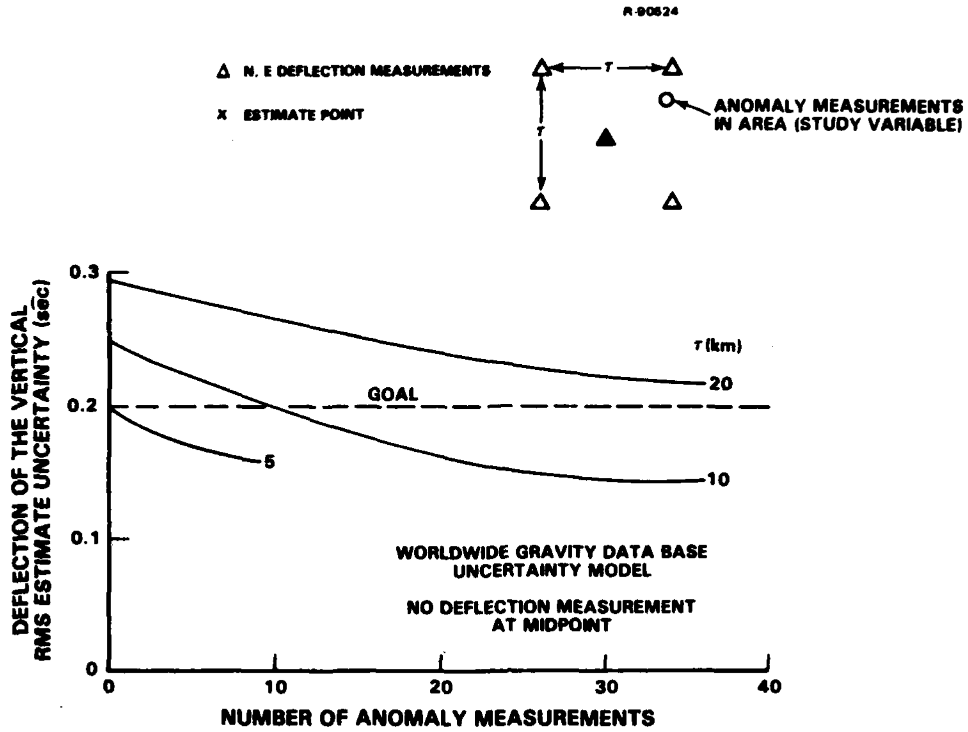

Figure 2.5-3 Alternative Astrogravimetric Measurement Strategies with Midpoint Deflection Measurement

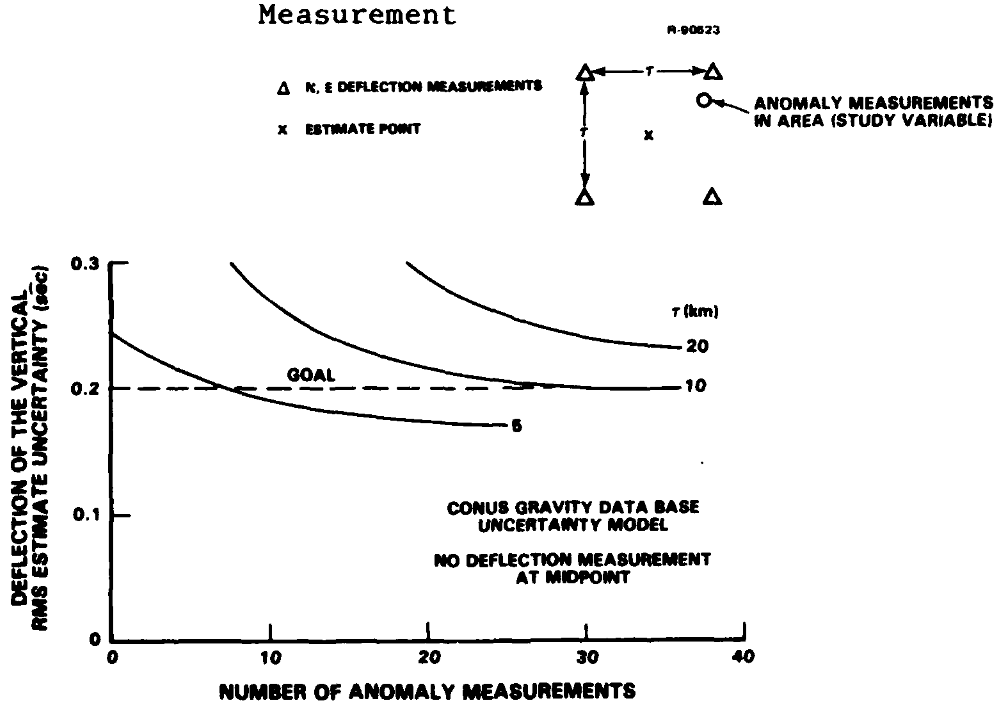

Figure 2.5-4 Alternative Astrogravimetric Measurement Strategies without Midpoint Deflection Measurement

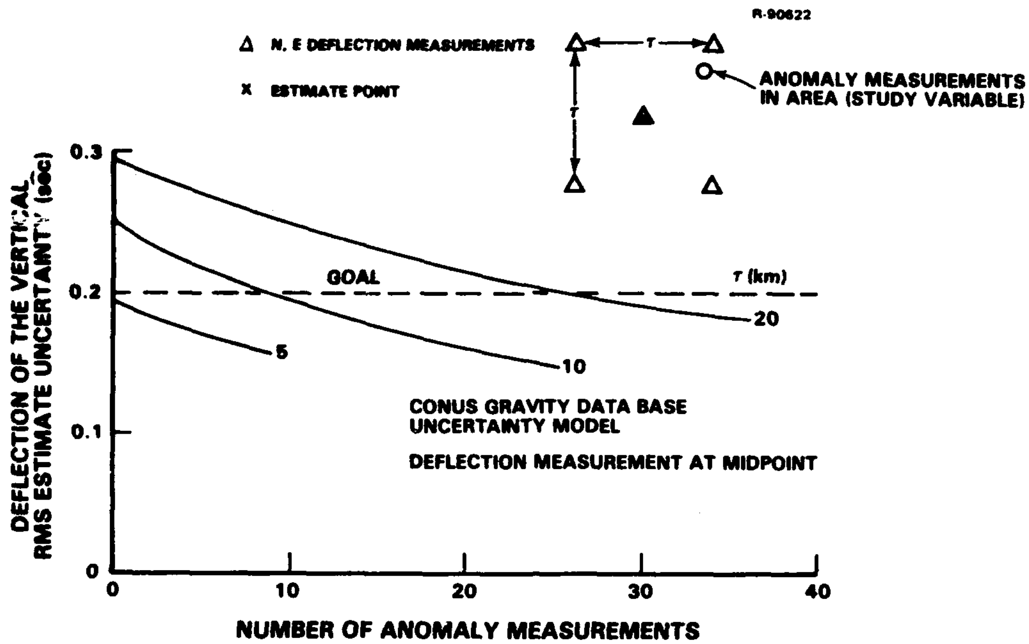

Figure 2.5-5 Alternative Astrogravimetric Measurement Strategies with Midpoint Deflection Measurement

For a given set of survey parameters, the CONUS area and data base results in estimation accuracies similar to those derived from the worldwide field. This is not surprising since the measurement densification of the survey models studied here greatly exceeds the average densification of existing worldwide or CONUS data.

3. ASTROGEODETIC/MOVING BASE INERTIAL SYSTEM SURVEYS

3.1 INTRODUCTION

In this chapter the deflection estimation accuracy achievable by optimally combining data from inertial systems and astrogeodetic measurements is explored. A major output of this effort is a formulation to combine multitrack data from moving base inertial systems, along with the astrogeodetic measurements, to "re-estimate" deflections of the vertical on the separate survey tracks in a post survey regional adjustment. The astrogeodetic measurements serve as endpoint calibration values for the baseline helicopter traverse studied herein. *This work is a direct continuation* of the covariance studies made in Ref. 1 for a single traverse of an inertial surveying configuration. The baseline error models (gravity, sensor, etc.) and the survey parameters of Ref. 1 are retained for use here.

Three types of moving base inertial systems are simulated for making accuracy potential comparisons. They are

1) a conventional inertial system typified by the RGSS (the baseline of Ref. 1)
2) a gradiometer-aided inertial system (the Bell configuration is modeled)
3) the Northrop NAS-26 astroinertial navigation system.

The NAS-26 utilizes a star-tracker, integral with the navigator, for making frequent star sightings to calibrate the gyros and

bound the position error. Although not configured for gravity surveys, the NAS-26 hardware is currently available. Some software and a zero velocity update capability would have to be added for survey use. The gradiometer-aided system is not presently available for use in gravity surveys, but the ability of a gradiometer configuration to estimate deflections of the vertical is assessed for future survey planning.

3.2 SIMULATION MODELS

The gravity disturbance field model, the navigation error model, and the sensor error models used here are identical to those of Ref. 1 wherein single track results are reported. Major characteristics of these models are listed here for completeness and reference. Also, the error model for the NAS-26 is described in the following.

3.2.1 Gravity Disturbance Model

The self-consistent third-order Markov model described in the previous chapter is utilized here to describe the statistics of the gravity disturbance field. However, as stated in Ref. 1, the parameters of the model have been adjusted to fit the White Sands gravity anomaly data to provide a gravity model that is representative of that region. The parameters, rms gravity anomaly and characteristic distance, are presented in Table 3.2-1. The Markov gravity disturbance model is used in its velocity-invariant (any vehicle velocity can be simulated) state-space form for covariance analysis, and contains the structure necessary to formulate the gravity gradients needed to model the gradiometer measurements. Details of the gravity model can be found in Appendix B of Ref. 1.

TABLE 3.2-1
WHITE SANDS GRAVITY MODEL PARAMETERS

PARAMETER	VALUE	UNITS
Anomaly rms, σ_g	15.8	mgal
Characteristic distance, β^{-1}	17.9	km

3.2.2 Navigation System Error Model

The main components of an inertial surveying system are gyros, accelerometers, a stabilized platform, support electronics, power supplies, environmental protection, and the appropriate software to compute, using sensed accelerations, the position and velocity of the carrying vehicle. The error equations for a full three-axis unaided inertial navigation system are given below. The position, velocity, and misalignment errors, coordinatized in the local-level frame (North, East, Down) are driven by accelerometer errors, gravity disturbances, and gyro drifts.

$$\delta\dot{\underline{r}} = \delta\underline{v} - \underline{\omega}_{EL} \times \delta\underline{r} \tag{3.2-1}$$

$$\delta\dot{\underline{v}} = \underline{u} - \delta\underline{g} - \underline{\psi} \times \underline{A} - (\underline{\omega}_{IL} + \underline{\Omega}) \times \delta\underline{v} \tag{3.2-2}$$

$$\dot{\underline{\psi}} = -\underline{\omega}_{IL} \times \underline{\psi} + \underline{\varepsilon} \tag{3.2-3}$$

where

$\delta\underline{r}$ = position error (computed-minus-true)

$\delta\underline{v}$ = velocity error (computed-minus-true)

$\underline{\psi}$ = misalignment (platform-to-computer)

$\delta\underline{g}$ = gravity error (true-minus-reference)

$\underline{A}$ = specific force; i.e., vehicle acceleration due to all forces acting except gravity (ideal accelerometer output)

$\underline{\Omega}$ = angular rate of earth-fixed axes with respect to inertial space

$\underline{u}$ = accelerometer error

$\underline{\varepsilon}$ = gyro drift

$\underline{\omega}_{IL}$ = angular rate of the local-level frame (L) with respect to inertial space (I)

$\underline{\omega}_{EL}$ = angular rate of the local-level frame with respect to earth (E)

Endpoint calibration accuracies for the survey traverse simulations are listed in Table 3.2-2. These accuracies, used at both the beginning and the end of the traverse simulation, model optimal endpoint calibration procedures. Position errors are stated relative to a local benchmark. Further discussion of endpoint initialization and termination values is given in Ref. 1.

TABLE 3.2-2
ENDPOINT CALIBRATION DATA

PARAMETER	VALUE	UNITS
Deflection of the Vertical	0.2	$\widehat{\text{sec}}$
Endpoint Gravity Acceleration	0.1	mgal
Relative Position Error	1.0	cm
Zero Velocity Error	0.002	km/hr

The state-space form of the error equations allows straightforward measurement and update implementations for zero velocity updates (ZUPTS), gradiometer measurements, the star sightings, and endpoint calibration procedures. The expanded (scalar) form of the navigation error equations are presented in Appendix A of Ref. 1.

3.2.3 Sensor Error Models

Gyroscopes and accelerometers are the major components of an inertial positioning system and contribute random errors to the quantities estimated. An error model for the inertial sensors is used in this study and integrated with the system error model.

Baseline Sensors - An initial random bias drift and a white noise drift are used to model the gyro errors. The parameters selected for these models reflect the quality of present-day production gyros. Values are given in Table 3.2-3. Discussion is provided in Ref. 1.

First-order Markov models are employed to simulate accelerometer bias instability and scale factor errors. A white noise accelerometer error is also included. The Markov terms account for the moderately rapid, yet bounded, error growth. White noise adequately models platform jitter, loop rebalance noise, and other high-frequency errors.

For the survey system employing a gravity gradiometer triad, a first-order Markov and a white noise error model are used to represent the self-noise effects of each of the gradiometers. Parameter values of the models may be chosen to simulate either the Bell or Draper gradiometer configurations. Models for the Bell system are documented here. They typify

TABLE 3.2-3
BASELINE SENSOR ERROR MODELS

SENSOR	MODEL DESCRIPTION	VALUE	UNITS
Gyroscope	Bias Drift	0.003	deg/hr
	White Noise Drift	0.003 (after one hour)	$deg/hr^{3/2}$
	Bias Instability-Markov		
Accelerometer	Initial Value	2	μg
	Time Constant	0.5	hr
	Scale Factor-Markov		
	Initial Value	1.5	ppm
	Time Constant	0.5	hr
	White Noise	1.0	μg
Gradiometer (Bell)	Self-noise-Markov		
	Initial Value	49	Eotvos (E)
	Time Constant	2105	hr
	White Noise	86	E^2/Hz

the survey results to be expected with gradiometers (little difference is observed in deflection of the vertical estimation accuracy between the Bell or Draper systems for the scenarios described in Ref. 1). A summary of the baseline sensor error models is presented in Table 3.2-3.

NAS-26 Astroinertial Navigation System -- The NAS-26 astroinertial navigation system consists of an Inertial Measurement Unit (IMU) that includes an enclosed three-gimbal stable reference platform and a star tracker. The IMU is made up of two Kearfott Gyroflex Mod 2 two-degree-of-freedom dry-tuned rotor gyros and three Kearfott Model 2401 single-axis accelerometers. The entire platform assembly can revolve about a vertical axis in the base of the pitch gimbal. The star tracker is mounted on the three-gimbal inertial platform in such a manner as to allow rotation both in azimuth about a vertical

axis relative to the platform, and also in elevation about a horizontal axis. The instantaneous field-of-view of the telescope is 40 $\widehat{\text{sec}}$.

Astroinertial operation involves using frequent star sightings as navigation references. The ephemerides for 61 stars whose magnitudes range from -1.46 to +3.50 are stored in computer memory (and updated annually). Assuming cloud cover does not pose a problem, an average of three stars per minute may be tracked. Normally, six to ten stars are available at any given time and a minimum of two stars are available anywhere/anytime. An onboard Kalman filter processes the stellar angular measurements to estimate updates for the states included in the onboard filter model (e.g., position, velocity, tilt, heading, gyro drift, accelerometer bias, star tracker elevation bias). Thus, these stellar updates tend to bound navigation position errors and provide gyro drift rate compensation, resulting in signficantly improved inertial performance. For the study involving the NAS-26 navigation system, error models appropriate for the component instruments are used. The error model parameters for these sensors are shown in Table 3.2-4. Note that these models indicate sensor components of lower quality than the baseline inertial system discussed in the previous section. The star tracker is modeled at a sighting accuracy of one $\widehat{\text{sec}}$ rms per axis per measurement.

3.3 ACCURACY EVALUATION METHODOLOGY

In this section the estimation and the estimation error covariance equations are formulated for <u>multitrack</u> gravity data processing. The method, which is based on Gauss-Markov theory and spatial collocation, handles the multisensor/multitrack data (to be defined shortly) arrangements systematically, and ensures <u>minimum variance estimates</u> with respect to the

TABLE 3.2-4
NAS-26 SENSOR ERROR MODELS

SENSOR	MODEL DESCRIPTION	VALUE	UNITS
Gyroscope	Initial Drift Rate	0.05	deg/hr
	Drift Rate Noise (after 1 hr)	0.05	deg/hr
Accelerometer	Bias Instability-Markov		
	Initial Value	5	μg
	Time Constant	24	hr
	Scale Factor (Bias)	3	ppm
	White Noise (10 sec average)	1	μg
Star Tracker	White Noise	1	$\widehat{\text{sec}}$

data and the error models used. The error equations determine the accuracy improvement obtained in the single-track deflection estimates by employing the new formulation in a post-survey regional adjustment. The formulation also accounts for the astrogeodetic measurements at traverse endpoints.

The Gauss-Markov formula relates the estimates (deflection of the vertical in this study) to the separate track data

$$\underline{\hat{x}} = \begin{pmatrix} \underline{\hat{x}}_1 \\ \underline{\hat{x}}_2 \\ \vdots \\ \underline{\hat{x}}_N \end{pmatrix} = \Phi_{xz}\Phi_{zz}^{-1}\,\underline{z} = \Phi_{xz}\Phi_{zz}^{-1}\begin{pmatrix} \underline{z}_1 \\ \underline{z}_2 \\ \vdots \\ \underline{z}_N \end{pmatrix} \qquad (3.3\text{-}1)$$

where

ϕ_{xz} = cross-covariance matrix between $\underline{x}$ (truth quantities) and $\underline{z}$

ϕ_{zz} = covariance of $\underline{z}$

$\hat{\underline{x}}_i$ = estimates for i^{th} track

$\underline{z}_i$ = data for the i^{th} track

N = total number of tracks involved.

In this application the data are the smoothed estimates of the deflections of the vertical for the separate tracks. These quantities are "re-estimated" based on data from nearby tracks. The covariance of the estimation errors of $\hat{\underline{x}}$ ($\tilde{\underline{x}} = \hat{\underline{x}}-\underline{x}$) are determined from

$$\phi_{\tilde{x}\tilde{x}} = \phi_{xx} - \phi_{xz}\,\phi_{zz}^{-1}\,\phi_{zx} \tag{3.3-2}$$

where ϕ_{xx} is the a priori (reference) covariance.

To describe the mechanics of the estimation procedure several matrices are required. The matrix ϕ_{xz} relates the reference field deflections to the single-track deflection estimates

$$\phi_{xz} = E(\underline{x}\underline{z}^T) = \begin{bmatrix} E(\underline{x}_1\underline{z}_1^T) & E(\underline{x}_1\underline{z}_2^T) & \cdots & E(\underline{x}_1\underline{z}_N^T) \\ E(\underline{x}_2\underline{z}_1^T) & \ddots & & \vdots \\ \vdots & & \ddots & \vdots \\ E(\underline{x}_N\underline{z}_1^T) & \cdots & \cdots & E(\underline{x}_N\underline{z}_N^T) \end{bmatrix} \tag{3.3-3}$$

where E is the ensemble expectation operator. The matrix ϕ_{zz} is the covariance matrix of the single-track deflection estimates

$$\phi_{zz} = E(\underline{z}\underline{z}^T) = \begin{bmatrix} E(\underline{z}_1\underline{z}_1^T) & E(\underline{z}_1\underline{z}_2^T) & \cdots & E(\underline{z}_1\underline{z}_N^T) \\ E(\underline{z}_2\underline{z}_1^T) & \ddots & & \vdots \\ \vdots & & \ddots & \vdots \\ E(\underline{z}_N\underline{z}_1^T) & \cdots & \cdots & E(\underline{z}_N\underline{z}_N^T) \end{bmatrix} \tag{3.3-4}$$

To define the submatrices needed for ϕ_{xz} and ϕ_{zz}, expressions relating the reference quantities with the single-track estimates are needed. Two forms prove to be useful in developing a mathematically and computationally tractable formulation of the multiple track smoothing problem. The first is

$$\underline{z}_i = \underline{x}_i + \underline{\eta}_i \qquad \text{(Estimate = Truth + Error)} \tag{3.3-5}$$

where $\underline{\eta}_i$ is the error in the i^{th} single-track estimates. Through optimal smoothing of the single-track data (including ZUPTS, gradiometer measurements, or star sightings) the covariance between the estimate, $\underline{z}_i$, and its error, $\underline{\eta}_i$, is zero. Thus, the covariance equation associated with Eq. 3.3-5 is

$$R_i = \Sigma_i - P_i \tag{3.3-6}$$

where

$R_i = E(\underline{z}_i\underline{z}_i^T)$ = covariance of the i^{th} single-track estimates

$\Sigma_i = E(\underline{x}_i\underline{x}_i^T)$ = covariance of the raw gravity field deflections on the i^{th} track

$P_i = E(\underline{\eta}_i\underline{\eta}_i^T)$ = covariance of the i^{th} track estimation errors

A state-space covariance simulation of the errors of a moving base inertial system (a fixed-point smoothing algorithm is included) is used to generate P_i. The reference field statistics, Σ_i, are known a priori from the Markov gravity model.

The second expression (referred to as the "data equation") relating the single-track estimates to the truth values is

$$\underline{z}_i = D_i \underline{x}_i + \underline{e}_i \tag{3.3-7}$$

where $\underline{e}$ is an error that is orthogonal to $\underline{x}_i$ (the covariance between $\underline{x}_i$ and $\underline{e}_i$ is zero). The matrix D_i is computed from

$$D_i = I - P_i \Sigma_i^{-1} \tag{3.3-8}$$

where I is the identity matrix.

The covariance of the a priori deflections may be represented by

$$\phi_{xx} = \begin{bmatrix} \Sigma_1 & C_{12} & \cdots & C_{1N} \\ C_{21} & \Sigma_2 & \cdots & C_{2N} \\ \vdots & & \ddots & \vdots \\ C_{N1} & \cdots & & \Sigma_N \end{bmatrix} \tag{3.3-9}$$

where C_{ij} is the cross-covariance of the deflections between tracks i and j. The cross terms approach zero as the tracks become widely separated.

Using the expressions listed in Eqs. 3.3-5 to 3.3-9, the expectation operations in Eqs. 3.3-3 and 3.3-4 are carried out to yield

$$\phi_{xz} = \begin{bmatrix} R_1 & C_{12}\,D_2^T & \cdots & C_{1N}D_N^T \\ C_{21}D_1^T & R_2 & & \vdots \\ \vdots & & \ddots & \vdots \\ C_{N1}D_1^T & \cdots & & R_N \end{bmatrix} \qquad (3.3\text{-}10)$$

and

$$\phi_{zz} = \begin{bmatrix} R_1 & D_1C_{12}D_2^T & \cdots & D_1C_{1N}D_N^T \\ D_2C_{21}D_1^T & R_2 & & \vdots \\ \vdots & & \ddots & \vdots \\ D_NC_{N1}D_1^T & \cdots & & R_N \end{bmatrix} \qquad (3.3\text{-}11)$$

Note that since the between-track correlations of the a priori deflections approach zero as the track separation increases, the dimensionality of the problem can be maintained at a tractable level by incorporating data from nearby tracks only. Processing data from remote tracks offers little accuracy improvement. Note that appropriate quantification of "remote" can be established by simulation. Examples are provided in the next section.

3.4 NUMERICAL RESULTS

The improvement in deflection estimation accuracy achievable by combining single-track deflection of the vertical estimates from moving base inertial systems, along with the astro-measurements, is reported here. Such results are indicative of the benefits derived from a post survey regional adjustment (data reduction process) based on the formulation described in the previous section. The example case used involves two parallel tracks with the separation distance varied

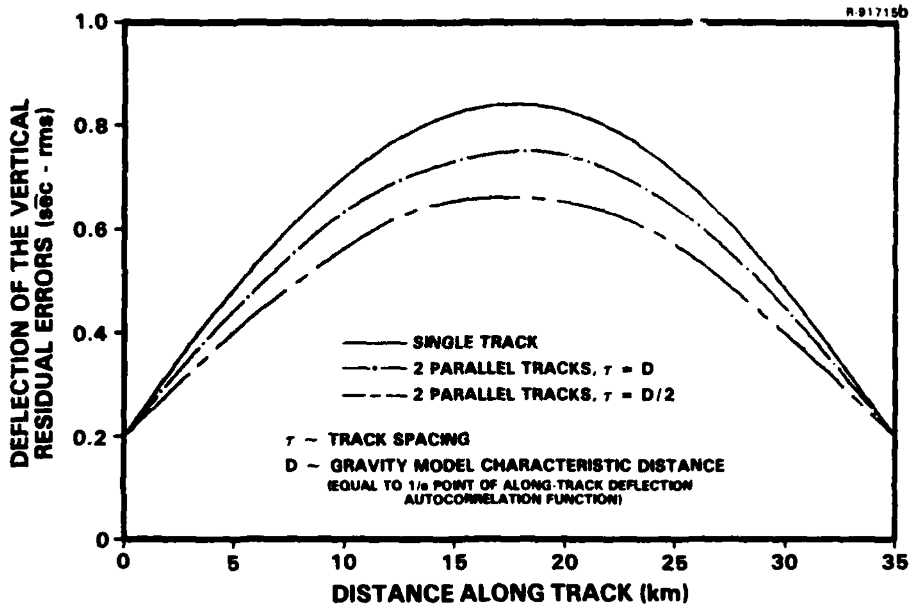

Figure 3.4-1 Accuracy Potential of Conventional Inertial System Two-Track Survey

as a parameter. Accuracy results for the three systems simulated, a conventional inertial system, a gradiometer-aided system, and the NAS-26 astroinertial system, are presented and discussed. Deflection of the vertical estimation accuracy is presented in graphs which also indicate the corresponding single-traverse accuracy found in Ref. 1. North deflection of the vertical post-survey residual rms error performance (the direction transverse to the track direction) is presented in the following paragraph. Improvement in the along-track components of the deflection (in this case, East) with multiple survey tracks, is somewhat smaller.

Note, in Fig. 3.4-1, that no improvement occurs at the traverse endpoints. This is to be expected for the single-track traverse since the inertial survey system provides <u>relative</u> deflection information, i.e., the deflection change from an endpoint value. Although a completely error free survey would

link endpoints as two effectively collocated measurements, the inertial system accuracies corresponding to the results in Fig. 3.4-1 are insufficient to provide a significant amount of endpoint coupling. A counter example, illustrating a case wherein the effective endpoint coupling is noticeable, is presented in Fig. 3.4-2.

For the multiple track cases in Fig. 3.4-1, the 0.2 $\widehat{sec}$ endpoint deflection accuracies also do not improve. This is due to the recognition that a vertical deflection station of this accuracy would usually be the result of a previous regional adjustment of deflection data. This was taken into account in the simulation study by treating the endpoint deflection errors for adjacent tracks as fully correlated.

For the estimation accuracy potential of a conventional moving base inertial system presented in Fig. 3.4-1, the baseline gyro and accelerometer error models, summarized in Table 3.2-3, are used. ZUPTs are performed at 4 minute intervals until the end of the survey. Figure 3.4-1 indicates the deflection of the vertical estimation uncertainty as a result of optimally combining data from <u>two parallel tracks</u>. This example is chosen for its simplicity and illustrates the variation of accuracy with track separation. The processing method, however, is applicable for any reasonable number of tracks with no inherent geometry restraints. The tracks run from West to East so that the North deflection is the cross-track component. Note that the smoothing operation, which utilizes all survey measurements in forming an estimate at any point in the survey, ensures a near symmetric error profile. The highest uncertainty occurs at the middle of the traverse, farthest from the calibrated endpoints. The results show a significant improvement with respect to the single-traverse accuracy depending on the track separation distance. Closer track spacing yields better accuracy. Also, the degradation in accuracy as the tracks are

separated is clearly seen. This is due to the decreasing spatial correlation of the gravity field.

The Bell gradiometer error model is integrated with the baseline navigation system and sensor error models to simulate an astrogeodetic/gradiometer-aided inertial system survey scenario. Endpoint calibration data, survey length, cruise velocity, and the gravity disturbance model remain unchanged. No ZUPTs are performed. Note from the performance indicated in Fig. 3.4-2 that ZUPTs are not needed for deflection survey-related gradiometer operations.

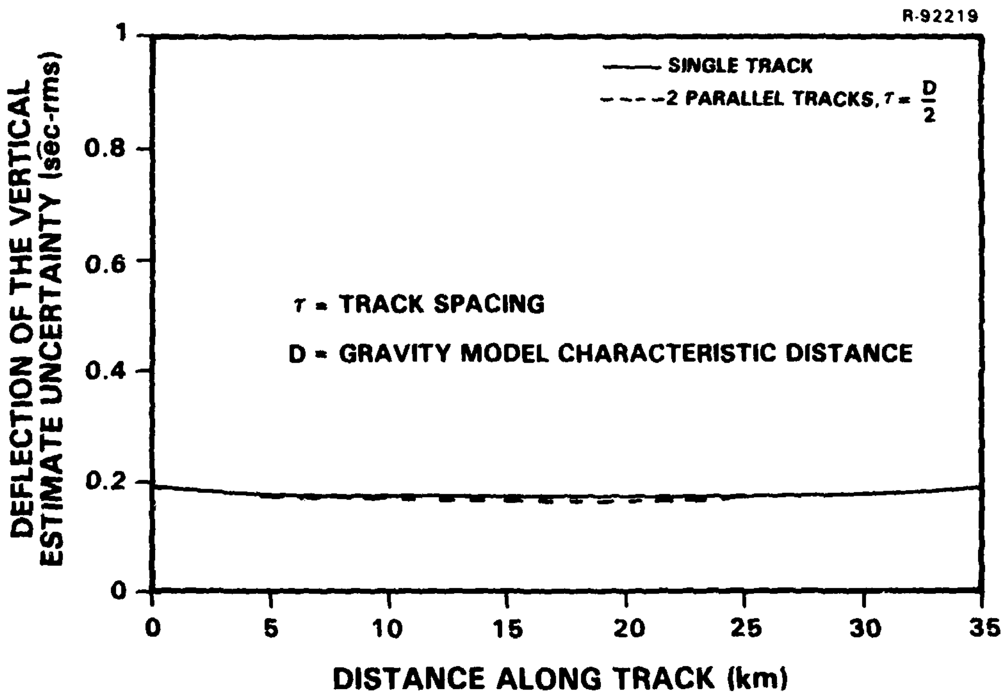

Figure 3.4-2 Accuracy Potential of Gradiometer-Aided Inertial System Two-Track Survey

In computing the post survey deflection of the vertical error residuals for the parallel track geometry, it was found that the single-traverse accuracy derived from the gradiometer-aided system could not be significantly improved by mixing data from tracks as close as 8.95 km, one-half the gravity disturbance characteristic distance. This is shown in Fig. 3.4-2.

The gradiometer, being a highly accurate and precise interpolator, in effect carries the astrogeodetic endpoint measurements along the entire traverse with a minimum of error. Little is gained by performing post survey regional adjustments on data collected by gradiometer-aided inertial systems. Of course, adjustment of the endpoint deflection stations according to the procedures outlined in Ref. 2 could offer the additional improvements indicated by a separate regional deflection station adjustment.

The survey scenario for the NAS-26 simulation mimicked that for the conventional inertial system case. ZUPTs were performed at 4 minute intervals. However, star sightings were also modeled and took place every 20 seconds. The accuracy improvement obtained by combining deflection estimates is presented in Fig. 3.4-3. In comparison with the conventional system results of Fig. 3.4-1 the NAS-26 single-track estimates are better. This is a result of the ability of the NAS-26 to finely calibrate the gyros in real time using the star sighting information. Since gyro errors are a major contributor to the bowed error profile of Fig. 3.4-1, as reported in Ref. 1, the elimination of such errors results in the flattened curve in Fig. 3.4-3. Accordingly, the accuracy improvement realized by combining NAS-26 data from two parallel tracks is not as marked as that observed from the conventional inertial system. This is not surprising since there is less error to be improved

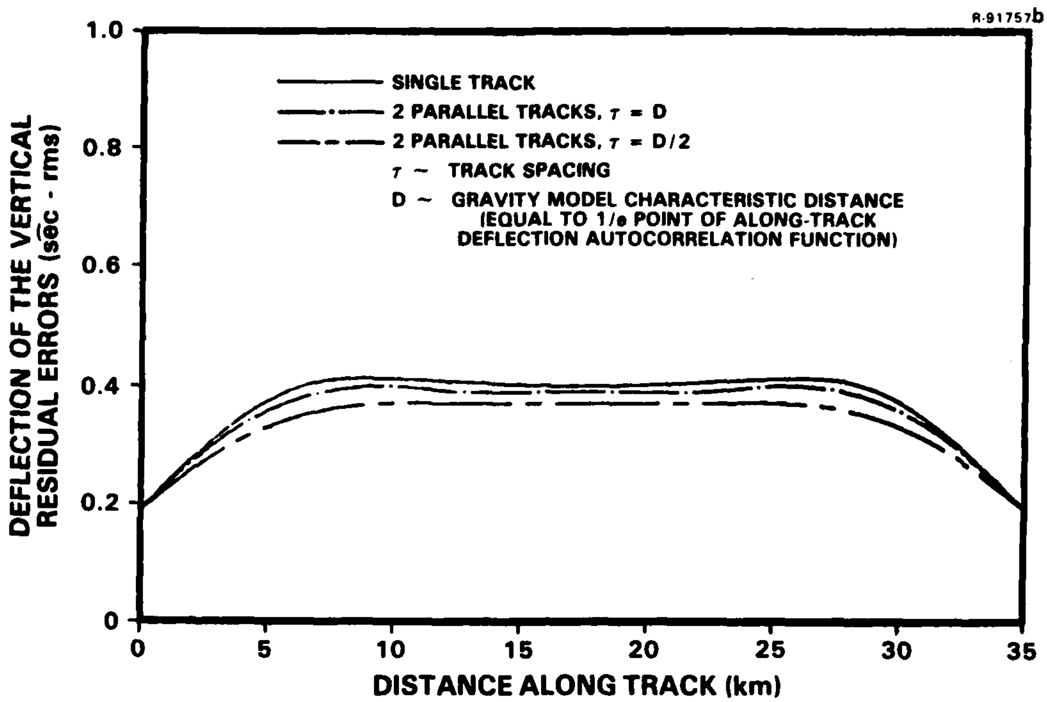

Figure 3.4-3 Accuracy Potential of NAS-26 Two-Track Survey

upon. Using the error models and survey scenario described in this effort, the NAS-26 astroinertial navigator is found to yield deflection estimates of intermediate accuracy in comparison to that obtained by conventional and gradiometer-aided inertial systems.

4. COSTS AND LOGISTICS

In this chapter assessments of relative costs and operational considerations, such as survey time, are presented for the system configurations analyzed. Accuracy comparisons are made using the results presented in previous chapters.

Astrogeodetic measurements of the deflection of the vertical must be made to achieve the high accuracy (0.2 $\widehat{sec}$) desired from modern surveys. The measurements are time-consuming, however, requiring a skilled crew to take one night or more per measurement. Therefore, such data is intended to supplement other measurement procedures and aid in lowering deflection of the vertical residual errors. In Chapter 2 it was shown that gravimeter measurements, which are simpler and less time-consuming to make, combined with astrogeodetic measurements, yield estimation uncertainties dependent on the spacing of the astrogeodetic measurements and the number of gravimeter measurements, with the potential of achieving high accuracies. Optimal processing methodology is used in assessing the tradeoffs. Since astrogeodetic and gravimetry technology is mature, little technical risk is incurred by taking this approach to survey a given area. Incremental productivity gains may be realized.

Inertial and gradiometric surveys performed on the ground or in the air offer higher survey productivity and can utilize infrequent astrogeodetic "benchmark" data in the processing algorithms. Despite optimal processing and post survey regional adjustments involving two tracks, conventional inertial surveys have difficulty reaching deflection of the vertical estimation accuracies of 0.2 $\widehat{sec}$. Inertial systems, however,

have reached a high level of positioning precision and are readily available. As mentioned in Ref. 1 such systems could be used to provide accurate positional data for surveys involving a gradiometer, which can provide very accurate deflection of the vertical estimates given astrogeodetic endpoint data. High development and procurement costs are associated with gradiometers, and they have yet to be fully demonstrated in prototype testing. Therefore, greater technical risk follows the use of a gradiometer.

The Northrop NAS-26 astroinertial navigation system, presently not used for other than experimental gravity data surveying, appears to estimate deflections of the vertical well. Marginal improvements in estimation accuracy are found when analyzing a two-track survey. The successful operation of the NAS-26 is dependent on weather conditions (clear skies), and added software would be necessary to handle ZUPTs and gravity data processing.

Figure 4-1 sketches the relative costs vs accuracy of various multisensor combinations. Multiple tracks are illustrated to increase survey costs for a given system configuration (through increased survey effect). The gradiometer configuration exhibits the highest accuracy, with correspondingly high costs. The astrogravimetric approach could be especially attractive in areas where considerable anomaly data is available. Further study identifying specific candidate locations for test surveys or astrogravimetric processing of existing data is needed.

The trends illustrated in Fig. 4-1 provide indications of the relative costs of different options for precise deflection of the vertical surveying. Detailed consideration of cost and logistical factors, of course, is a multidimensional problem in its own right, with few overall value measures which

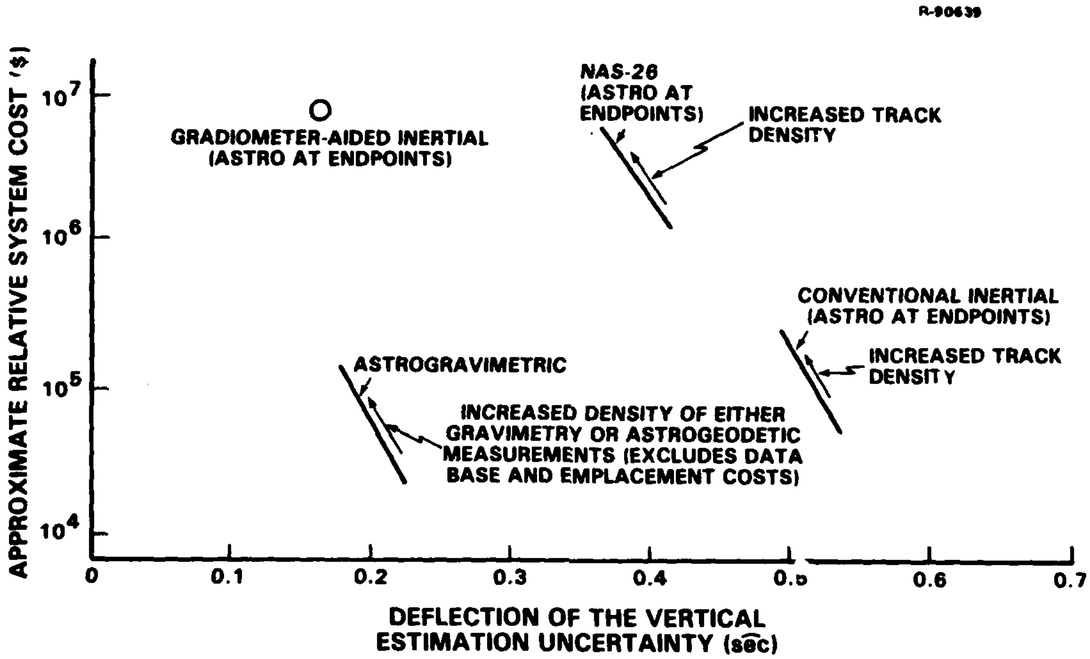

Figure 4-1 Order of Magnitude Cost-Accuracy Comparison of Multisensor Technologies

are universally accepted. Although a complete and detailed study of all such factors is beyond the resources of this study, Tables 4-1 and 4-2 present several significant considerations for each class of surveying approach. Of course each option listed in the table could be pursued in several variant forms. For example, the different remedial procedures and processes discussed in Ref. 2 can be applied to T-4 Theodolite-based astrogeodetic surveys. Similarly, inertial surveying system gyros and accelerometers can be replaced with more sensitive components. While such refinements of the main technological thrusts in deflection surveying are important, they typically provide single benefits such as more accuracy, lower cost, more efficiency, etc. Since the incremental improvement offered by such refinement technology is usually straightforward to assess, Tables 4-1 and 4-2 instead address alternative approaches which span different technologies.

SURVEY APPROACHES	DATA TYPE (AFTER REDUCTION)	KEY HARDWARE INVOLVED	APPROXIMATE SYSTEM ACCURACY (sec)	APPROXIMATE SYSTEM ACQUISITION COST	APPR[illegible]XIMATE COST PER DATA [illegible] OR TRACK [illegible] ACQUISITION AN[illegible] OTHER [illegible]	[illegible]
Conventional Astro-geodetic Survey	Vertical Deflections	Theodolite (T-4 or similar)	0.3	$60K	[illegible]	[illegible]
Astrogeodetic Survey	Deflections	Astrolobe (Danjon or similar)	0.3	[illegible]	[illegible] estimate	[illegible]
Astrogeodetic Survey	Deflection	T-4 with CCD eyepiece	0.2-0.3	$100K (eyepiece system only)	[illegible] estimate	[illegible]
Astrogeodetic Survey	Deflections	Astrolabe with CCD eyepiece and TCR	0.1-0.2	$[illegible]K-500K (full system)	[illegible] (estimate)	one night
Gravimetric Survey	Free Air Anomalies	Gravimeter (BGM-2 or L&R Model G)	0.2-0.5	$25K (excludes Vening Meinesz software)	$50-$100 (estimate)	one hour [illegible] are re[illegible] deflect[illegible]
Astrogravimetric Survey	Deflections/ Anomalies	Theodolites/ Gravimeters	0.2-0.3	$125K (excludes anomaly and deflection combination software)	$50-$150 (estimate)	[illegible]eral hours (average - estimated for moderately sized survey)

TABLE 4-1

COST AND LOGISTICS CONSIDERATIONS FOR ALTERNATIVE FIXED STATION TECHNIQUES TO DETERMINE DEFLECTIONS OF THE VERTICAL

TIME TO ACQUIRE ONE POINT OR TRACK OF DATA (EXCLUSIVE OF PROCESSING)	EFFORT REQUIRED TO PROCESS MEASUREMENTS INTO DEFLECTION ESTIMATES	TIME TO TRAIN SURVEY PERSONNEL	REQUIRED FUTURE DEVELOPMENT/ IMPROVEMENT POTENTIAL	COMMENTS
one night	significant, several hours per point	several months or more	mature, in place .	current standard technology
one night	moderate, one hour per point	several weeks	hardware available procedures require development	no standard operating procedure for field use
one night	moderate, one hour per point	several weeks to a few months	some hardware development required; some risk (processing software poses low risk	key contributions due to accuracy data processing advances; prototype system currently available, improved version in 1-4 years
one night	moderate, computer intensive, one hour of technician time per point (estimated)	one month	to be developed; key technologies now available, modest risk	probable five year development cycle
one hour (many points are required for one deflection estimate)	significant, involves Vening Meinesz equations; several months for software setup	several days	mature, in place technology	indicated accuracy assumes use of current worldwide and CONUS data bases
several hours (average - estimated for moderately sized survey)	significant, requires software development (months)	same as for astro and gravimetric surveys separately	available; survey integration required	technique offers potentially modest cost and data acquisition time benefits

SURVEY APPROACHES	DATA TYPE (AFTER) REDUCTION	KEY HARDWARE INVOLVED	APPROXIMATE SYSTEM ACCURACY (sec)	APPROXIMATE SYSTEM ACQUISITION COST	APPROXIMATE COST PER DATA POINT OR TRACK (EXCLUDING ACQUISITION AND OTHER ONE TIME COSTS)	TIME TO ACQUIRE ONE POINT OR TRACK OF DATA (EXCLUSIVE OF PROCESSING)
Surface or Helicopter Inertial Survey (with endpoint deflection values given)	deflections over the traverse	inertial survey system (RGSS, IPS-2)	0.5	$500K-$1.0M (full system)	$100-$300	four hours (automotive, 30-60 km traverse)
Surface or Helicopter Inertial Survey using daytime star tracker	Deflection over the traverse	Inertial system, star tracker (NAS-26)	0.35	$800K†	$100-$300 (estimate)	four hours (30-60 km traverse)
Surface or Helicopter Inertial/Gradiometer Survey	Deflection over the traverse	initial system, gradiometer system	0.1-0.2	$10M-$20M (full system)	$100-$300 (estimate)	one hour (30-60 km traverse)
Fixed Wing Aircraft Gradiometer Survey	Deflections over large survey areas (500 km×500km typical)	aided inertial/ gradiometer	0.2	$10M-30M (full system, except aircraft)*	Dominated by aircraft operations cost - 2000 tracks required for typical large survey area	(four hours per 500 km track)

*Includes estimate of development costs

†$600K likely in late 1984.

TABLE 4-2

COST AND LOGISTICS CONSIDERATIONS FOR ALTERNATIVE MOVING BASE TECHNIQUES TO DETERMINE DEFLECTIONS OF THE VERTICAL

INT ING THER)	TIME TO ACQUIRE ONE POINT OR TRACK OF DATA (EXCLUSIVE OF PROCESSING)	EFFORT REQUIRED TO PROCESS MEASUREMENTS INTO DEFLECTION ESTIMATES	TIME TO TRAIN SURVEY PERSONNEL	REQUIRED FUTURE DEVELOPMENT/ IMPROVEMENT POTENTIAL	COMMENTS
	four hours (automotive, 30-60 km traverse)	modest using available software, several hours	several weeks	in place, modest improvement potential	key improvements will be associated with use of additional sensors
	four hours (30-60 km traverse)	requires software development (1-2 yrs), operational data reduction modest (several hrs)	one-two months	hardware in place, potential has been demonstrated, modest risk	requires primarily software development and testing
	one hour (30-60 km traverse)	moderate - requires processing gradient data into deflections; operational data reduction expected modest (several hrs)	one-two months	demonstrated at-sea; land system under development, some technical risk	no ZUPTs required; five year development cycle
- ks ical a	(four hours per 500 km track)	high - requires accuracy continuation and several years of software development; operational data reduction expected to treat typical large survey area in several weeks	one-two years (initially)	airborne survey development program in planning stages only - some technical risk	will require more than five years to develop unless accelerated

4.1 CONVENTIONAL ASTROGEODETIC SURVEY

Conventional theodolite surveys, discussed in detail in Ref. 6, are the current mainstay of deflection of the vertical determination in the United States. The technology is mature and the tradeoffs among alternative data reduction methodologies are well understood. The key disadvantage with the astrogeodetic method is the inherent difficulty of using a theodolite to provide astronometric data consistent with 0.2 arcsecond accuracy. This element is indicated in Table 4-1 both in the time required to train surveying personnel (note that many in the community view several months as an optimistic estimate of the apprenticeship period for a first-order astro surveyor) and the time and cost needed to obtain a single astrogeodetic station. Cost estimates given in the table are based on discussions with members of the surveying community.

4.2 ASTROLABE-BASED DEFLECTION SURVEYS

Recent interest in using astrolabes for deflection determination has arisen primarily as a response to the training and observation time requirements for conventional theodolite surveys. The key justification for the consideration of astrolabes is the more relaxed training and observing regime. In Table 4-1, a Danjon astrolabe is considered as typifying field portable instrumentation. "Field portable" is used in the same sense as often applied to the Wild T-4 theodolite. Although not easily handled, a party of two can manage the equipment on all except the most inhospitable terrain. Pricing information is estimated with the note that the Danjon astrolobe is no longer made, and no predictable second-hand market exists. However discussions with various user community members indicate the amount given in Table 4-1 is a reasonable guess at costs.

Since the number of astrolabes available at any given time is likely to be low, any large scale or quick-response survey requirement which would be addressed using astrolabes would likely be subject to manufacturing or procurement delays of several years. Alternatively if custom instruments were built, or a new production facility opened, the cost of a dozen or so astrolabes produced on an accelerated basis could easily reach a unit cost more than an order of magnitude higher than given in Table 4-1.

4.3 T-4 WITH CHARGE COUPLED DEVICE (CCD) EYEPIECE

The CCD eyepice is a technology which promises modest accuracy improvements (reduces human observer-induced measurement uncertainty) and significant productivity increases. Costs indicated in Table 4-1 would add to amounts needed for the theodolite and yet-to-be developed production survey computer software. The decreased cost per data point (versus conventional astrosurvey) indicated in Table 4-1, is estimated to be gained largely through data processing efficiencies and reduction in the amount of rejected data.

4.4 ASTROLABE WITH CCD EYEPIECE AND TWO COLOR REFRACTOMETER (TCR)

This developmental technology promises significant accuracy and productivity improvements beyond current T-4 performance through the elimination of observer uncertainty, control of refraction effects and utilization of the astrolabe's efficiency. The system cost estimates of Table 4-1 are based on the procurement of hardware for a prototype; they exclude costs for development of supporting computer software and testing costs.

4.5 GRAVIMETRIC SURVEY

Gravimetric surveys, while not generally as accurate for deflection of the vertical generation as astrogeodetic techniques, are attractive because of the relatively low equipment costs, ease of use and survey productivity limited essentially by how fast the gravimeter can be transported from site to site. Of course, although the cost per gravity anomaly point is low, it must be kept in mind that the processing effort required to transform gravity data into deflections is considerable. For subarcsecond accuracy, not only are many gravimetric measurements required near each deflection point (inner zone densification) but the processing must be coordinated with regional and worldwide data base holdings to properly account for distant zone weighting. Although exceptions have been noted (see Ref. 2)*, gravimetry alone is generally not considered viable for high accuracy deflection determination in the CONUS.

4.6 ASTROGRAVIMETRIC SURVEY

The key promise of the astrogravimetric method is the relaxation of astro densification requirements through interpolation using less costly gravimetric measurements. As indicated in Table 4-1, the results of the present study indicate that desired area-wide survey accuracies can be achieved with an astrogravimetric approach. However, less clear is whether, in actual survey practice, astrogravimetric surveying would offer a significant cost or time savings over an astro survey of equivalent accuracy. Definitive answers could be provided

*Also, currently-used launch region gravity model techniques for certain land-based ICBMs utilize a variant of the gravimetric method.

either by an intensive directed study or implementation of a proto survey. The latter would require a significant commitment to computer software development for data integration. The indicated acquisition costs assume the use of one gravimeter and one T-4 or equivalent theodolite.

4.7 SURFACE OR HELICOPTER INERTIAL SURVEY

This category in Table 4-2 describes current inertial survey technology. Costs per track of data are driven primarily by field crew and equipment maintenance costs, (assuming high annual utilization rates).* The key advantage of inertial survey approaches, or any other moving-base technique, is rapid data gathering, amenability to automation and a minimal need for personnel with highly specialized skills. Note that, while the accuracy indicated in Table 4-2 does not meet the 0.2 $\widehat{sec}$ goal, additional improvements to inertial survey systems are possible. These are detailed and evaluated in Ref. 1. One such improvement is discussed in the next paragraph.

4.8 INERTIAL SURVEY USING A STAR TRACKER

The only currently-available system utilizing this aided-inertial configuration is the NAS-26 prototype. Although some development would be required to tranform this system into a production survey configuration, certain test results as well as the simulation studies described earlier in this report are encouraging. As indicated in Table 4-2, current

*For example, taking a five year amortization of a one million dollar acquisition and spares cost, adding fifty thousand dollars of average annual finance charges and assuming 100 traverses per year of utilization, gives a capital cost alone of $250 per traverse.

hardware costs would decrease once the system, now baselined for B-1 test instrumentation, is in full production. Although the survey accuracy indicated in Table 4-2 is not at goal levels, improvements such as those discussed in Ref. 1 are possible. One particularly effective expedient, of course, is to increase, to the extent possible, deflection calibration accuracy of traverse terminal points.

4.9 INERTIAL/GRADIOMETER SURVEY

The gravity gradiometer, now under development with DMA sponsorship, has already demonstrated laboratory performance sufficient to reach the accuracy levels indicated in Table 4-1. At-sea tests have verified ruggedness. However, several years of applied development await production survey utilization of gradiometer systems. Nonetheless, when operational, the economics and logistics of their utilization should be nearly equivalent to those of conventional inertial survey equipment.

4.10 FIXED WING AIRCRAFT GRADIOMETER SURVEY

The long term potential of the gradiometer as a rapid survey tool is efficiently exploited by using a fixed wing aircraft as the host vehicle. Although well into the future, current data suggest that, for surveying very large regions quickly, the very high development and acquisition costs for an airborne gradiometric survey system could be worthwhile. Key technical risks lie in the areas of successful system integration of existing technology and aircraft, and the implementation of techniques to process the very large volumes of data returned by an airborne gradiometric sensor. An additional potential benefit of an airborne gradiometer system is its applicability to broad ocean areas as well as over land.

4.11 OVERALL PERSPECTIVE

Tables 4-1 and 4-2 supports several observations

- Technologically advanced alternatives to conventional astrogeodetic surveys can provide considerably increased deflection data acquisition capability at current first-order accuracies or better. However, these alternatives have associated research and acquisition costs which tend to increase exponentially with capability. These costs may be justifiable in terms of per unit deflection data cost if alternative new systems are heavily utilized.

- Astrogeodetic survey techniques, especially those involving astrolabe use, updated to include automated observing and more computerized data reduction offer marked relief from traditional difficulties in training and data quality assurance. Order of magnitude improvements in data acquisition rates, however, are unlikely due to star viewing time constraints.

- The costs of developing and maintaining an automated or semiautomated astrogeodetic technology base are modest compared with those associated with advancing moving-base survey techniques.

- Economic benefits associated with utilizing astrogravimetric methods may be realizable but modest.

- Moving-base methods, the only feasible approaches to densifying deflection data over large areas (e.g., all CONUS coastlines, new multi-state areas, etc.) within a reasonable timespan, are within reach using presently-available technology. The cost and risk of this technique vary in approximate proportion to the ultimate survey accuracy and speed offered.

- The recurrent technical risk theme in most alternative deflection measurement schemes is the development of computer software. Although the software needs of most candiate sensors are easily addressed, little has been done toward integrating the widespread survey data (or even organizing its acquisition) which will be provided by new alternative techniques. These new measurements, which will be obtained on a large scale at sub arcsecond accuracies, must be integrated into existing data bases without loss of information. In addition, this processing must be accomplished without overloading the mapping community's ability to perform the necessary data reductions. Software and data base techniques, similar to those embodied in the present DoD gravity anomaly library and DMA weapon support systems, are needed at the instrument/field level to prepare for the future availability of very accurate and highly densified deflection of the vertical measurements.

- A relatively low cost (when compared to the cost of moving base survey hardware development) interim approach to maintaining a deflection survey "breakout" capability for the next five-to-ten years would be to simply proliferate astrolabe-trained observers, acquire instruments and initiate a data acquisition program. Such an approach could adequately address deflection of the vertical requirements for strategic weapons systems where the data needs are restricted to limited areas and also for many tactical needs. Examples include deflection initialization stations, aircraft inertial systems, vertical deflection references at government test sites and independent deflection sites used as survey tie points.

5. SUMMARY AND CONCLUSIONS

Alternative multisensor deflection of the vertical survey approaches were examined which offer promise of approaching or bettering an accuracy goal of 0.2 $\widehat{sec}$. Specific techniques studied and their projected performance include:

- Gravimetric Enhancement of Astrogeodetic Data Fields - The astrogravimetric approach offers a survey design "tradeoff" in which many gravimetric measurements can be substituted for a few astrogeodetic stations. However, a minimum number of astro measurements is always required to reach deflection accuracy goal levels. This number varies with proximity of the deflection estimate to a location where a deflection observation is available. The astro site spacing also varies with the accuracy of both the astrogeodetic and gravimetric data and the correlation distance of the gravity field. Typical deflection and anomaly measurement densities, which offer goal level deflection accuracy, range from no gravity anomaly measurements and an astro site spacing of 5 km to an anomaly spacing of 1.7 km with an astro spacing of 15 km.

- Regional Adjustment of Conventional Inertial Survey Traverses Using Astrogeodetic Endpoint Data - Post-survey adjustment of inertial survey measurements, using optimum smoothing techniques, offers deflection accuracy improvements over single track traverses up to 20% per additional data track. However the accomplishment of goal level accuracies is still difficult. Using conventional inertial technology (e.g., RGSS) and two 35 km parallel tracks, mid-traverse deflection recovery is 0.6 $\widehat{sec}$ rms.

- Regional Adjustment of NAS-26 Quality, Inertial Survey Traverses - Post-survey adjustment of NAS-26 survey data offers modest improvement beyond single track accuracies. For traverses between 15 and 35 km long, typical midpoint deflection accuracy is near 0.4 $\widehat{sec}$ rms.

- Regional adjustment of Gravity Gradiometer Survey Traverses - The gradiometer effectively replicates the deflection endpoint accuracy at all traverse points. Regional adjustment of gradiometer traverse data provides negligible deflection recovery improvement behond that obtainable by optimally smoothing each traverse.

The formulation for combining multisensor/multitrack data from moving base inertial system surveys for gravity data estimation is a major product of this effort. The methodology is general in terms of allowable measurement types and track arrangements. Future work should focus on such cases as crossing track and repeat traverse scenarios. Most importantly, the methodology should be used to process actual RGSS data to realize, at the earliest possible date, the benefits of the approach.

The information presented in Tables 4-1 and 4-2 provides a capsule summary of major deflection survey alternatives. These alternatives include both single optical sensor approaches as well as integrated multisensor methods.

This study, as well as two earlier related studies (Refs. 1 and 2), supports the following conclusions:

- Technologically advanced deflection of the vertical survey systems now under development offer promise of 0.2 $\widehat{sec}$

accuracy or better, as well as relief from the time constraints now associated with acquiring deflection data.

- Only modest relief can be expected from the current cost of high accuracy deflection of the vertical stations.

- Efficient utilization of new deflection of the vertical survey approaches accents the need to direct resources toward automation. Particular attention to the development and operation of software and computer support systems will be especially needed.

Further study is recommended toward the effective organization and utilization of deflection of the vertical data. Considerable new amounts of data of sub-arcsecond accuracy will become available as the techniques described in this and earlier reports (e.g., Refs. 1 and 2) are implemented.

APPENDIX A
SEQUENTIAL COLLOCATION FORMULAS

Sequential collocation offers a convenient method of processing measurement data from one sensor at a time in an estimation problem in which several sensors may be involved. Processing multisensor data sequentially reveals the impact each sensor has on estimation accuracy. Complex iteration algorithms are available in the literature (Ref. 5) for implementing the sequential collocation technique. For convenience the sequential collocation estimation and estimation error covariance formulas are listed in this Appendix for three measurement types.

A.1 PROBLEM FORMULATION

It is desired to estimate a vector quantity $\underline{X}$ given measurements of $\underline{u}$, $\underline{v}$, and $\underline{w}$. A measurement of $\underline{X}$ itself may be made, and correlations may, of course, exist among any of the quantities. The dimensions of the vectors need not be equal. As an example, suppose it is required to estimate deflections of the vertical in a given survey area wherein gravity anomaly and undulation measurements are available. These three quantities are correlated to some degree, and an appropriate gravity disturbance model is used to describe the covariance structure of the variables. For example, collocation formulas could be used to estimate the deflections and their associated uncertainty using the anomaly measurements alone and then in conjunction with undulation measurements.

Table A-1 defines the notation used in the formulation. Note that $C_{ab}^{T} = C_{ba}$.

TABLE A-1

NOTATION AND NOMENCLATURE FOR COLLOCATION FORMULAS

$\hat{\underline{X}}_{abc}$	= estimate of $\underline{X}$ given measurements of $\underline{a}$, $\underline{b}$, and $\underline{c}$
$\underline{Z}_a$	= noisy measurement of $\underline{a}$ ($\underline{a} + \underline{\eta}_a$)
R_a	= covariance of $\underline{\eta}_a$
$C_{ab.cde}$	= covariance of $\underline{a}$ and $\underline{b}$ given measurements of $\underline{c}$, $\underline{d}$, and $\underline{e}$.

A.2 SEQUENTIAL COLLOCATION FORMULAS

In Table A-2 the formulas for the first estimate of $\underline{X}$ and its associated error covariance matrix, given the measurements $\underline{Z}_u$ of the first sensor, are presented. These are familiar expressions in minimum variance estimation. Given the measurements $\underline{Z}_v$ of the second sensor, the estimate and its error covariance matrix are calculated as shown in Table A-3. Note that in a state-space format new measurement (H) and measurement noise (R) matrices would be brought in to perform the update. However, using collocation, the computation of conditional covariance matrices is necessary. In particular, the results of the first update are needed in the computation of the second. Continuing the process, the results of utilizing $\underline{Z}_v$ are embodied in the formulas of Table A-4. These formulas process the final measurements, $\underline{Z}_w$.

TABLE A-2

COLLOCATION FORMULAS FOR
FIRST MEASUREMENT TYPE

$$\hat{\underline{X}}_u = C_{xu}[C_{uu} + R_u]^{-1}\,\underline{Z}_u$$

$$C_{xx.u} = C_{xx} - C_{xu}[C_{uu} + R_u]^{-1}\,C_{ux}$$

TABLE A-3

COLLOCATION FORMULAS FOR
SECOND MEASUREMENT TYPE

$$\hat{\underline{X}}_{uv} = \hat{\underline{X}}_u + C_{xv.u}(C_{vv.u} + R_v)^{-1}[\underline{Z}_v - C_{vu}[C_{uu} + R_u]^{-1}\underline{Z}_u]$$

$$C_{xx.uv} = C_{xx.u} - C_{xv.u}[C_{vv.u} + R_v]^{-1}\,C_{vx.u}$$

where

$$C_{xv.u} = C_{xv} - C_{xu}[C_{uu} + R_u]^{-1}\,C_{uv}$$

$$C_{vv.u} = C_{vv} - C_{vu}[C_{uu} + R_u]^{-1}\,C_{uv}$$

TABLE A-4

COLLOCATION FORMULAS FOR
THIRD MEASUREMENT TYPE

$$\hat{\underline{X}}_{uvw} = \hat{\underline{X}}_{uv} + C_{xw.uv}(C_{ww.uv} + R_w)^{-1}\,\underline{Z}_w - C_{wv.u}(C_{vv.u} + R_v)^{-1}[Z_v - C_{vu}(C_{uu} + R_u)^{-1}\underline{Z}_u]$$

$$C_{xx.uvw} = C_{xx.uv} - C_{xw.uv}[C_{ww.uv} + R_w]^{-1}\,C_{wx.uv}$$

where,

$$C_{xw.uv} = C_{xw.u} - C_{xv.u}(C_{vv.u} + R_v)^{-1}\,C_{vw.u}$$

$$C_{ww.uv} = C_{ww.u} - C_{wv.u}(C_{vv.u} + R_v)^{-1}\,C_{vw.u}$$

$$C_{xw.u} = C_{xw} - C_{xu}(C_{uu} + R_u)^{-1}\,C_{uw}$$

$$C_{wv.u} = C_{wv} - C_{wu}(C_{uu} + R_u)^{-1}\,C_{uv}$$

$$C_{ww.u} = C_{ww} - C_{wu}(C_{uu} + R_u)^{-1}\,C_{uw}$$

The above sequential collocation procedure is computationally equivalent to the straightforward batch formulation of Table A-5. In Table A-5 all sensor measurements are processed at once to yield the final estimate vector and its error covariance matrix. The effects of the individual sensors cannot be seen. Although a large matrix must be inverted in the batch scheme (and precludes using this approach for a very large number of measurements)* no real computational savings are realized in the sequential algorithm due to the added complexity of computing the conditional covariance matrices. Its main advantage is the conceptual, sensor-specific clarity it offers.

TABLE A-5

COLLOCATION BATCH SCHEME FOR THREE MEASUREMENT TYPES

$$\hat{\underline{X}}_{uvw} = [C_{xu}\ C_{xv}\ C_{xw}] \begin{bmatrix} C_{uu}+R_u & C_{uv} & C_{uw} \\ C_{vu} & C_{vv}+R_v & C_{vw} \\ C_{wu} & C_{wv} & C_{ww}+R_w \end{bmatrix}^{-1} \begin{bmatrix} \underline{Z}_u \\ \underline{Z}_v \\ \underline{Z}_w \end{bmatrix}$$

$$C_{xx.uvw} = C_{xx} - [C_{xu}\ C_{xv}\ C_{xw}] \begin{bmatrix} C_{uu}+R_u & C_{uv} & C_{uw} \\ C_{vu} & C_{vv}+R_v & C_{vw} \\ C_{wu} & C_{wv} & C_{ww}+R_w \end{bmatrix}^{-1} \begin{bmatrix} C_{ux} \\ C_{vx} \\ C_{wx} \end{bmatrix}$$

*For such situations the GEOFAST algorithm of Ref. 6 is appropriate.

APPENDIX B
ASTRONOMIC LATITUDE DETERMINATION WITH GYROSCOPIC SYSTEMS

ASTRONOMIC LATITUDE DETERMINATION WITH GYROSCOPIC SYSTEMS

ADDRESSED AS ONE OF SEVERAL ACTION ITEMS FROM ETL/TASC MEETING OF 19,20 AUGUST 1982.

R-92934

- <u>BASIC PRINCIPLE</u>:

  MOUNT A RATE GYRO ON A LEVEL PLATFORM WITH ITS INPUT AXIS POINTING APPROXIMATELY NORTH. ROTATE THE PLATFORM ABOUT THE VERTICAL AXIS UNTIL THE GYRO RATE OUTPUT, ω_M, IS A MAXIMUM. THEN

  $$\omega_M = \Omega \cos L_A$$

  AND

  $$L_A = \arccos \frac{\omega_M}{\Omega}$$

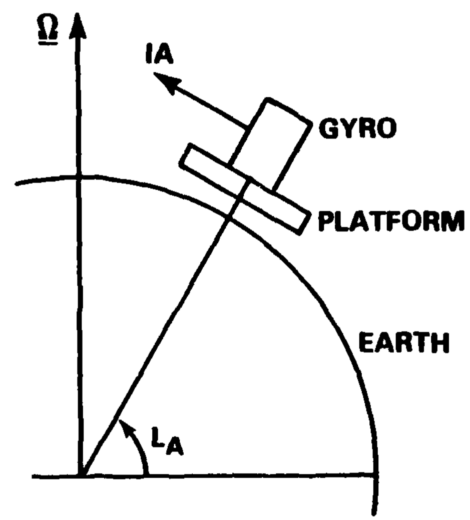

- SIMILAR INSTRUMENTATION EXISTS FOR AZIMUTH (AZIMUTH LAYING SET). ACCURACY IS SEVERAL $\widehat{sec}$.

- <u>ERROR SOURCES</u>:

  LEVELLING ACCURACY - REQUIRES SOME FORM OF LEVEL DETECTOR

  GYRO INPUT AXIS DEFINITION (RELATIVE TO LEVEL DETECTOR)

  GYRO DRIFT

  GYRO SCALE FACTOR ERROR

R-93019

ORIENTATION ERRORS

LEVELLING ACCURACY:

$$\frac{\partial L_{AM}}{\partial \phi_W} = 1, \text{ WHERE } \phi_W = \text{LEVELLING ERROR ABOUT THE WESTERLY AXIS}$$

(LEVEL DETECTOR ERROR OF ONE $\widehat{sec}$ CAUSES ONE $\widehat{sec}$ OF ASTRONOMIC LATITUDE ERROR)

GYRO INPUT AXIS DEFINITION LIMITS:

GYRO AND LEVEL DETECTOR CASE ALIGNMENT STABILITY ~ 0.5 $\widehat{sec}$, IF ADDRESSED CAREFULLY

INPUT AXIS ALIGNMENT STABILITY (ABOUT WEST) ACHIEVED IN LABORATORY ENVIRONMENT

- SDOF FLOATED (TGG): OF THE ORDER OF 0.5 $\widehat{sec}$ WITHIN A GIVEN POWER-ON CYCLE FOR PERIODS OF SEVERAL DAYS. MUCH LARGER OVER POWER CYCLES

- RING LASER GYRO: SMALL FRACTION OF AN ARC SECOND WHEN OPERATING. ON ORDER OF 0.5 $\widehat{sec}$ OVER POWER CYCLES

- FIELD CALIBRATION TECHNIQUES WOULD NEED TO BE DEVELOPED; SEVERAL APPROACHES OFFER PROMISE

R-93020

GYRO DRIFT

- VARIATION WITH LATITUDE

  $\delta L_A = \frac{\delta\omega}{\Omega \sin L_A}$ = ASTRO LATITUDE ERROR

  $\delta\omega$ = GYRO DRIFT RATE (SMALL)

- SERIOUS DIFFICULTIES NEAR EQUATOR ($L_A \rightarrow 0$)
- FOR $L_A = 45°$, $\delta\omega = 5 \times 10^{-5}$ deg/hr $\rightarrow$ 1.0 $\widehat{\sec}$
- FIELD CALIBRATION REQUIRED; SUB ARCSECOND ACCURACY STILL DIFFICULT
- DRIFT RATE ERROR CONTROL TECHNIQUES AVAILABLE

  CAROUSEL PLATFORM

  WHEEL SPEED MODULATION

R-93021

GYRO SCALE FACTOR ERROR

- VARIATION WITH LATITUDE

  $$\delta L_A = \varepsilon \cot L_A$$

  ε = SCALE FACTOR ERROR

- SIMILAR TO PROBLEM WITH DRIFT AT LOW LATITUDES

- FOR $L_A = 45°$, ε = 5 PARTS PER MILLION $\rightarrow$ 1.0 $\widehat{\text{sec}}$

R 93022

NET ASSESSMENT OF GYRO TECHNIQUE TO DETERMINE LATITUDE

- CURRENT STATE OF THE ART IS NEAR 1.0 $\widehat{sec}$
- BETTER ACCURACY REQUIRES SEVERAL PROBLEMS TO BE ADDRESSED
- SOLUTIONS APPEAR DIFFICULT BUT POSSIBLE
- MULTIPLE GYRO SYSTEM COULD PROVIDE SOME RELIEF FROM ERROR SOURCES
- POSSIBILITY OF PERFORMANCE NEAR 0.2 $\widehat{sec}$ REQUIRES FURTHER STUDY

APPENDIX C
TRANSLOCATION OF DEFLECTION MEASUREMENTS

TRANSLOCATION CONCEPT

GIVEN: ACCURATE DOV MASTER STATION
DIFFERENTIAL ASTRO MEASUREMENT BETWEEN MASTER AND REMOTE SITE

ESTIMATE: DOV AT REMOTE SITE USING OPTIMAL MINIMUM VARIANCE TECHNIQUES

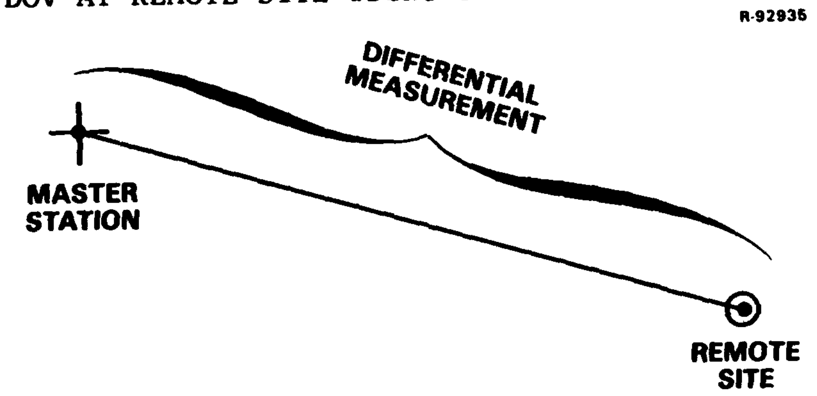

RATIONALE: DIFFERENTIAL DEFLECTION MEASUREMENTS CAN BE MORE ACCURATE BECAUSE OF COMMON MODE ERROR SOURCE CANCELLATION (e.g., REFRACTION)

PROBLEM: COMMON MODE PORTION OF DEFLECTION FIELD NOT OBSERVABLE

R-93015

STUDY CASE SUMMARY

- MASTER STATION EXTRAPOLATION ONLY - NO DIFFERENTIAL MEASUREMENT
- CONVENTIONAL INDEPENDENT ASTRO MEASUREMENT AT REMOTE SITE - NO DIFFERENTIAL MEASUREMENTS
- ACCURATE MASTER STATION PLUS INDEPENDENT DIFFERENTIAL MEASUREMENT
- ALONG-SHIFT DEFLECTION COMPONENT ADDRESSED
- DISTINGUISHES EFFECTS OF ERRORS DUE TO:
    - DIFFERENTIAL MEASUREMENT ERROR
    - GRAVITY FIELD DECORRELATION
- WHITE SANDS GRAVITY FIELD MODEL (σ = 2.4 $\widehat{\text{sec}}$, D = 18 km)
- DISTANCE BETWEEN MASTER STATION AND REMOTE SITE SCALED TO GRAVITY MODEL CHARACTERISTIC DISTANCE (D)

EXTRAPOLATION FROM MASTER STATION

R-92930

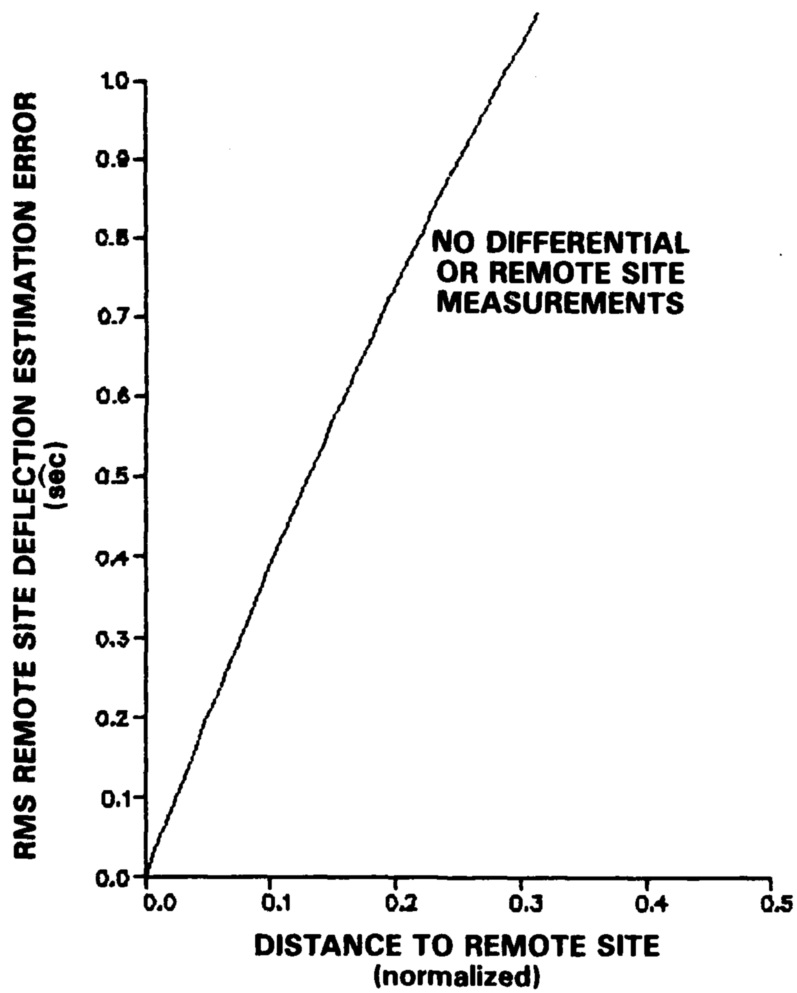

TRANSLOCATION USING IDEAL (ERROR-FREE) MASTER STATION

R-92932

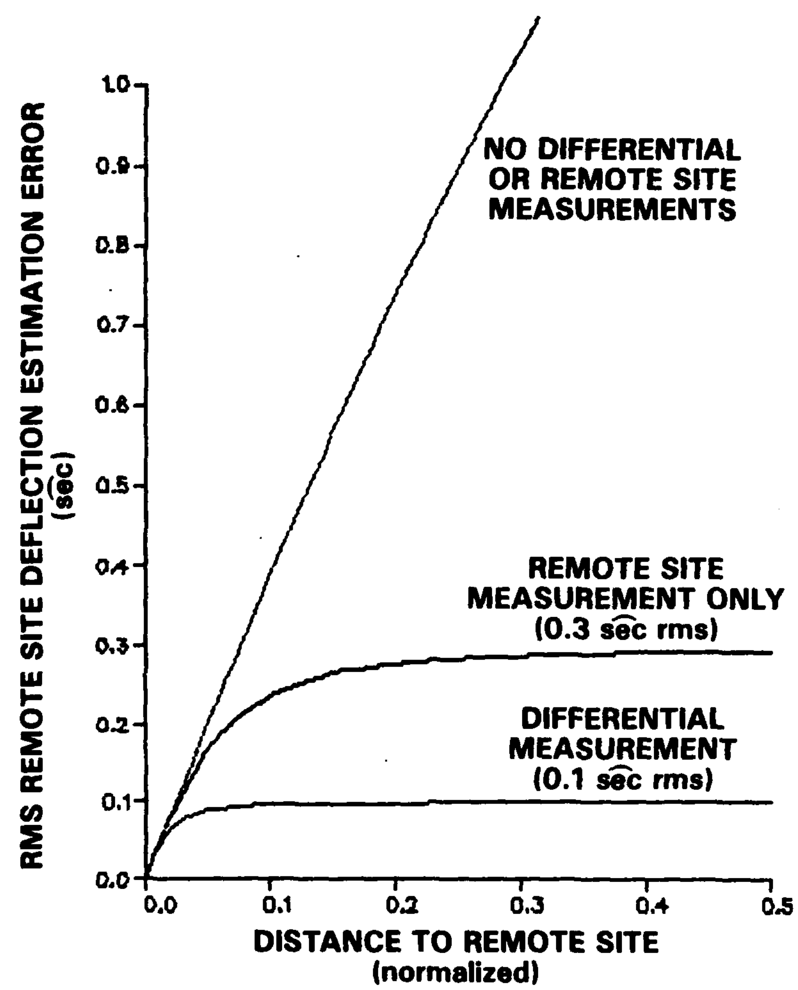

TRANSLOCATION USING VERY ACCURATE MASTER STATION
(0.1 $\widehat{sec}$ rms error)

R-92931

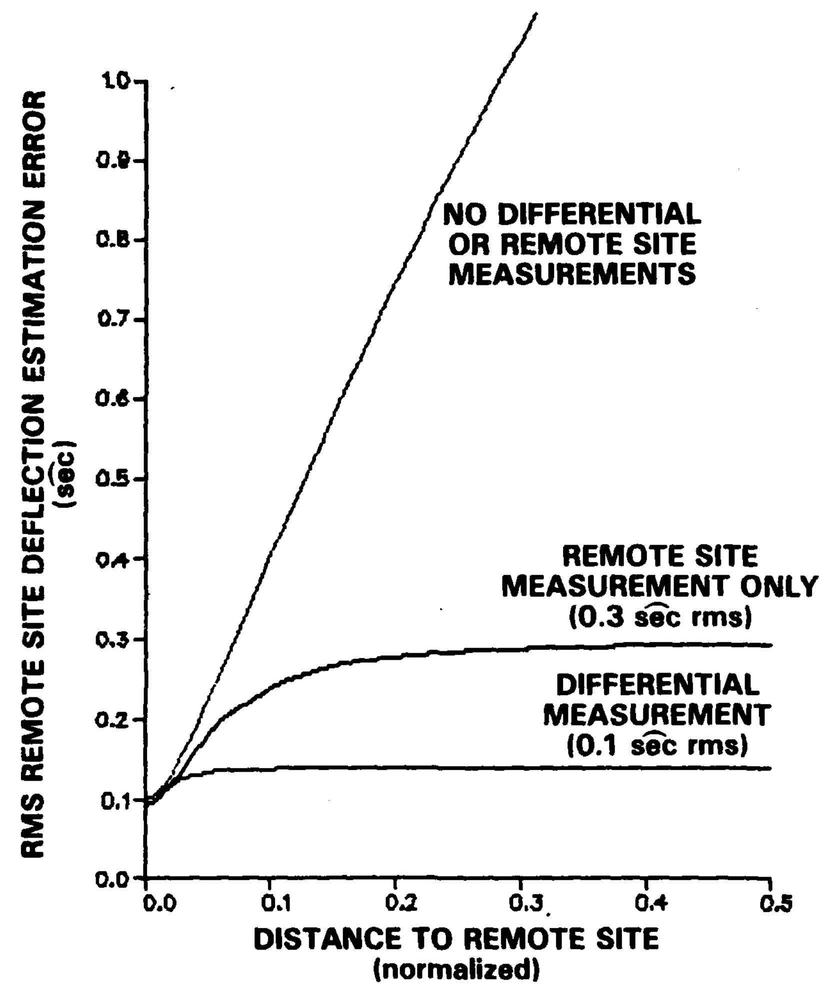

TRANSLOCATION USING MODERATE ACCURACY MASTER STATION

R-92933

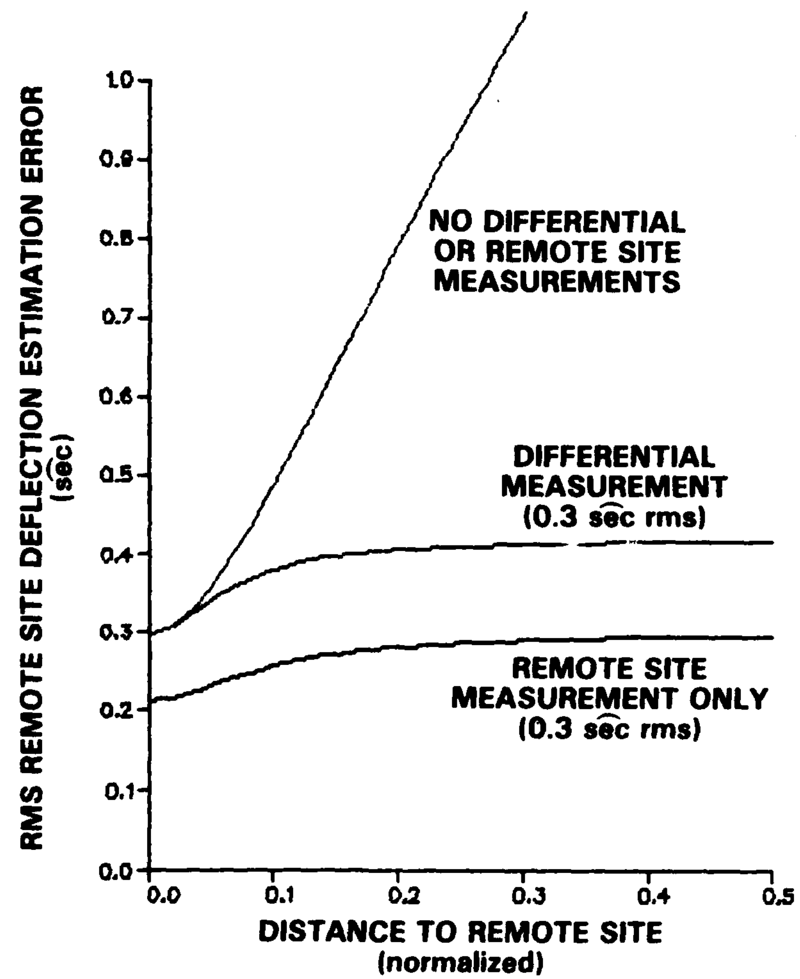

R-93016

ASTRO TRANSLOCATION OBSERVATIONS

- MASTER STATION EXTRAPOLATION ALONE DEGRADES ACCURACY TO 1.0 $\widehat{\text{sec}}$ WITHIN 25% OF A DEFLECTION CHARACTERISTIC DISTANCE

- CONVENTIONAL MEASUREMENTS AT REMOTE SITE ARE PREFERRED TO DIFFERENTIAL MEASUREMENTS <u>OF THE SAME ACCURACY</u>

- DIFFERENTIAL MEASUREMENT CAN BE ADVANTAGEOUS IF SIGNIFICANTLY (3:1) MORE ACCURATE

- GRAVITY FIELD CORRELATION EFFECTS DISAPPEAR* AT 50% OF THE CHARACTERISTIC DISTANCE

- ALLOW PREVIOUS RESULTS/MORE COMPLICATED TRANSLOCATION GEOMETRIES TO BE UNDERSTOOD

*FOR APPLICATIONS INVOLVING DOV TRANSLOCATION

R-93017

TRANSLOCATION CONCLUSIONS

- TECHNIQUE HAS POTENTIAL FOR MODEST ASTRO SURVEY ACCURACY IMPROVEMENT
- SIMILAR RESULTS CAN BE ACHIEVED THROUGH DENSIFICATION OF CONVENTIONAL OBSERVER STATIONS
- DIFFERENTIAL OBSERVATIONS OVER MODERATE DISTANCE (> 2 km) MUST BE MORE ACCURATE THAN CORRESPONDING CONVENTIONAL OBSERVATIONS TO REALIZE BENEFIT
- TECHNICAL BASIS FOR ACHIEVEMENT OF SIGNIFICANT DIFFERENTIAL ACCURACY BEYOND BEST CONVENTIONAL ASTRO MEASUREMENT ALTERNATIVES IS PROBLEMATIC

REFERENCES

1. Baumgartner, S.L., et al., "Assessment of Inertial Technology for Gravity Survey Applications," The Analytic Sciences Corporation, Technical Report ETL-0291, May 1982.

2. Heller, W.G., LeSchack, A.R., and Cushman, S.F., "Assessment of Means for Determining Deflection of the Vertical," The Analytic Sciences Corporation, Technical Report ETL-0303, August 1982.

3. Kahan, J.P. and Heller, W.G., "Utilization of Prototype Gravity Gradiometers for Surveying," The Analytic Sciences Corporation, Technical Report, TR-1946-9, January 1983.

4. Jordan, S.K., "Self-Consistent Statistical Models for the Gravity Anomaly, Vertical Deflections, and Undulation of the Geoid," Journal of Geophysical Research, Vol. 77, No. 20, July 1972.

5. Mortiz, H., "Stepwise and Sequential Collocation," Report No. 203, Dept. of Geod. Sci., Ohio State University, Columbus, Ohio, 1973.

6. Tait, K.S., "Generalized Fast Estimation Algorithm for Geodetic Applications," The Analytic Sciences Corporation, Technical Report TR-1946-7, January 1983.

7. Forsberg, R., and Tscherning, C.C., "The Use of Height Data in Gravity Field Approximation by Collocation," Journal of Geophysical Research, Vol. 86, No. B9, pp. 7843-7854, September 1981.